2. EXPLANATORY NOTES[1]

Shipboard Scientific Party[2]

Standard procedures for both drilling operations and preliminary shipboard analysis of the material recovered during Deep Sea Drilling Project (DSDP) and Ocean Drilling Program (ODP) drilling have been regularly amended and upgraded since drilling began in 1968. In this chapter, we have assembled information that will help the reader understand the basis for our preliminary conclusions and also help the interested investigator select samples for further analysis. This information concerns only shipboard operations and analyses described in the site reports in the *Initial Results* volume of the Leg 124 *Proceedings of the Ocean Drilling Program*. Methods used by various investigators for shore-based analysis of Leg 124 data will be detailed in the individual scientific contributions published in the *Scientific Results* volume.

AUTHORSHIP OF SITE CHAPTERS

The separate sections of the site chapters were written by the following shipboard scientists (authors are listed in alphabetical order in parentheses; no seniority is necessarily implied):

Site Summary (Rangin, Silver)
Background and Scientific Objectives (Rangin, Silver)
Geologic Setting (Rangin, Silver)
Operations (Foss, Jarrard, von Breymann)
Lithostratigraphy (Betzler, Brass, Huang, Linsley, Nichols, Pubellier, Smith, Solidum, Spadea)
Biostratigraphy (Müller, Nederbracht, Scherer, Shyu)
Paleomagnetics (Hsu, Merrill, Shibuya)
Sediment-Accumulation Rates (Hsu, Merrill, Müller, Nederbracht, Scherer, Shibuya, Shyu)
Sediment Inorganic Geochemistry (Sheu, von Breymann)
Organic Geochemistry (Berner, Bertrand)
Physical Properties (Lewis, Tannant)
Basement Lithology (Sajona, Smith, Spadea)
Basement Geochemistry (Sajona, Smith, Spadea)
Downhole Measurements (Brass, Jarrard)
Stress Measurements (Brass, Jarrard, Silver)
Seismic Stratigraphy (Rangin, Silver)
Summary and Conclusions (Shipboard Scientific Party)

Following the text of each site chapter are summary core descriptions ("barrel sheets" and igneous rock visual core descriptions) and photographs of each core.

DEFINITIONS

Many terms in this volume may be used in a format that is not familiar to the reader, or the usage here may differ from previous DSDP-ODP format. To make these terms more readily understandable, they are defined in this section.

Lithologic Units

During Leg 124 all lithologic units are labeled consecutively from the seafloor ("mudline") core down. The sediment lithologic units are designated by roman numerals (I, II,...), and the basement lithologic units are designated by arabic numerals (1, 2,...).

SURVEY DATA

Survey data collected prior to Leg 124 and used in the site selection process is discussed in a separate section (Site Survey Reports in Section 2), as well as in the seismic stratigraphy section for each site. The underway geophysical data collected aboard the *JOIDES Resolution* during Leg 124 are discussed in the Underway Geophysics chapter in Section 1. The underway data include bathymetry, magnetics, and seismic reflection profiles.

Drilling Characteristics

Water circulation down the hole is open, hence cuttings are lost onto the seafloor and cannot be examined. The only available information about sedimentary stratification in uncored or unrecovered intervals, other than from seismic data or wireline-logging results, is from an examination of the behavior of the drill string as observed and recorded on the drilling platform. Typically, the harder a layer, the slower and more difficult it is to penetrate. A number of other factors, however, determine the rate of penetration, so it is not always possible to relate drilling time directly to the hardness of the layers. Bit weight and revolution per minute, recorded on the drilling recorder, influence the penetration rate.

Drilling Deformation

When cores are split, many show signs of significant sediment disturbance, including the downward-concave appearance of originally horizontal bands, haphazard mixing of lumps of different lithologies (mainly at the tops of cores), and the near-fluid state of some sediments recovered from tens to hundreds of meters below the seafloor. Core deformation probably occurs during any of several steps in which the core may experience stresses sufficient to alter its physical characteristics: cutting, retrieval (with accompanying changes in pressure and temperature), and core handling on deck.

SHIPBOARD SCIENTIFIC PROCEDURES

Numbering of Sites, Holes, Cores, and Samples

ODP drill sites are numbered consecutively from the first site drilled by the *Glomar Challenger* in 1968. A site number refers to one or more holes drilled while the ship was positioned over one acoustic beacon. Multiple holes may be drilled at a single site by pulling the drill pipe above the seafloor (out of hole), moving the ship some distance from the previous hole, and then drilling another hole.

For all ODP drill sites, a letter suffix distinguishes each hole drilled at the same site. For example: the first hole drilled is assigned the site number modified by the suffix A, the second

[1] Rangin, C., Silver, E., von Breymann, M.T., et al., 1990. *Proc. ODP, Init. Repts.*, 124: College Station, TX (Ocean Drilling Program).

[2] Shipboard Scientific Party is as given in the list of participants preceding the contents.

hole takes the site number and suffix B, and so forth. Note that this procedure differs slightly from that used by DSDP (Site 1 through 624), but prevents ambiguity between site- and hole-number designations. It is important, for sampling purposes, to distinguish among holes drilled at a site, because recovered sediments or rocks from different holes usually do not come from equivalent positions in the stratigraphic column.

The cored interval is measured in meters below seafloor (mbsf). The depth interval assigned to an individual core begins with the depth below the seafloor that the coring operation began, and extends to the depth that the coring operation ended (see Fig. 1). For example, each coring interval is generally up to 9.7 m long; however, the coring interval may be shorter and may not necessarily be adjacent to each other, but may be separated by drilled intervals. In soft sediments, the drill string can be "washed ahead" with the core barrel in place, without recovering sediments. This is achieved by pumping water down the pipe at high pressure to wash the sediment out of the way of the bit and up the space between the drill pipe and wall of the hole. If thin, hard, rock layers are present, then it is possible to get "spotty" sampling of these resistant layers within the washed interval, and thus have a cored interval greater than 9.7 m. In drilling hard rock, a center bit may replace the core barrel if it is necessary to drill without core recovery.

Cores taken from a hole are numbered serially from the top of the hole downward. Core numbers and their associated cored intervals in meters below seafloor usually are unique in a given hole; however, this may not be true if an interval must be cored twice, due to caving of cuttings or other hole problems. Maximum full recovery for a single core is 9.7 m of rock or sediment contained in a plastic liner (9.5 m long, 6.6-cm internal diameter) plus about 0.2 m (without a plastic liner) in the core catcher (Fig. 2). The core catcher is a device at the bottom of the core barrel that prevents the core from sliding out when the barrel is being retrieved from the hole. In certain situations (e.g., when coring gassy sediments that expand while being brought on deck) recovery may exceed the 9.7-m maximum.

A recovered core is divided into 1.5-m sections that are numbered serially from the top (Fig. 2). When full recovery is obtained, the sections are numbered from 1 through 7 with the last section possibly being shorter than 1.5 m (rarely, an unusually long core may require more than seven sections). When less than full recovery is obtained, there will be as many sections as needed to accommodate the length of the core recovered; for example, 4 m of core would be divided into two 1.5-m sections and one 1-m section. If cores are fragmented (recovery less than 100%), sections are numbered serially and intervening sections are noted as void, whether shipboard scientists believe that the fragments were contiguous *in situ* or not. In rare cases a section less than 1.5 m may be cut to preserve features of interest (e.g., lithological contacts).

By convention, material recovered from the core catcher is placed below the last section when the core is described, and labeled core catcher (CC); in sedimentary cores, it is treated as a separate section. The core catcher is placed at the top of the cored interval in cases where material is only recovered in the core catcher. However, information supplied by the drillers or by other sources may allow for more precise interpretation as to the correct position of core-catcher material within an incompletely recovered cored interval.

A recovered rock (basalt, gabbro, or peridotite) core also is cut into 1.5-m sections that are numbered serially; however, each piece of rock is then assigned a number (fragments of a single piece are assigned a single number, with individual fragments being identified alphabetically). The core-catcher sample is placed at the bottom of the last section and is treated as part of the last section, rather than separately. Scientists completing

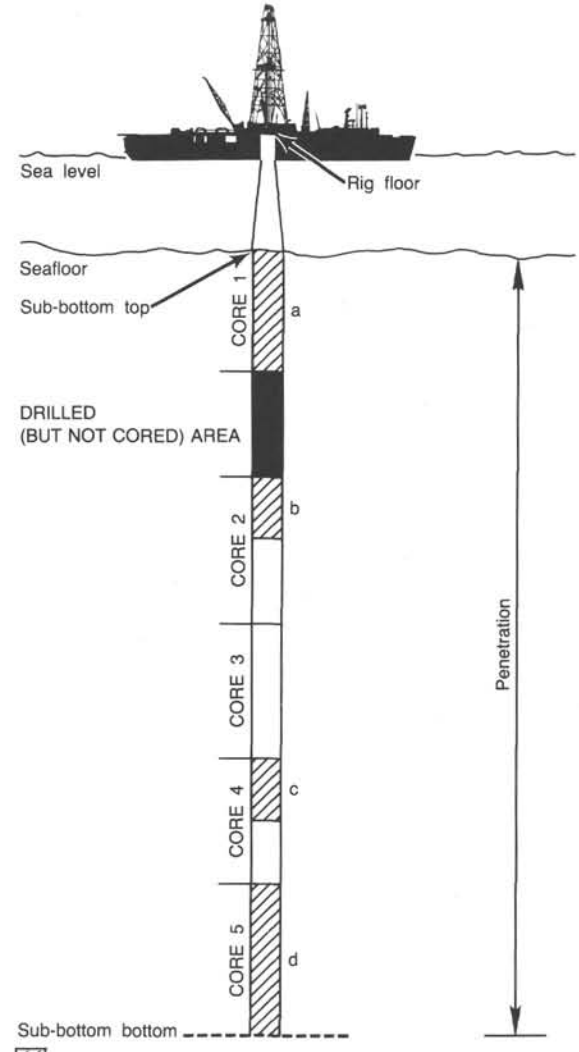

BOTTOM FELT: distance from rig floor to seafloor

TOTAL DEPTH: *distance from rig floor to bottom of hole* (sub-bottom bottom)

PENETRATION: distance from seafloor to bottom of hole (sub-bottom bottom)

NUMBER OF CORES: *total of all cores recorded,* including cores with no recovery

TOTAL LENGTH OF CORED SECTION: distance from sub-bottom top to *sub-bottom bottom minus drilled* (but not cored) areas in between

TOTAL CORE RECOVERED: total from adding a, b, c, and d in diagram

CORE RECOVERY (%): equals TOTAL CORE RECOVERED divided by TOTAL LENGTH OF CORED SECTION *times 100*

Figure 1. Core numbering and terms used in coring operations and core recovery.

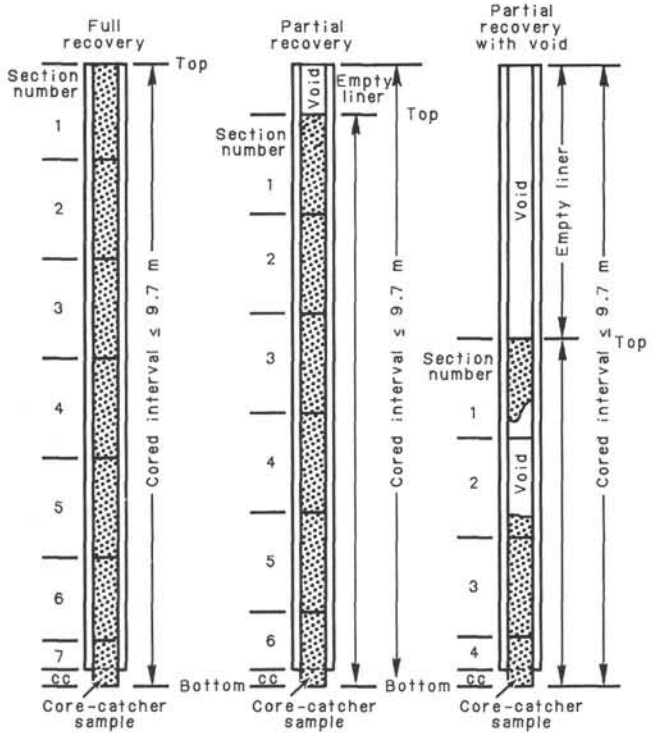

Figure 2. Examples of numbered core sections.

visual core descriptions describe each lithologic unit, noting core and section boundaries only as physical reference points.

When, as is usually the case, the recovered core is shorter than the cored interval, the top of the core is equated with the top of the cored interval by convention, to achieve consistency in handling analytical data derived from the cores. Samples removed from the cores are designated by distance measured in centimeters from the top of the section to the top and bottom of each sample removed from that section. In curated hard rock sections, sturdy plastic spacers are placed between pieces that did not fit together to protect them from damage in transit and in storage; therefore, the centimeter interval noted for a hard-rock sample has no direct relationship to that sample's depth within the cored interval, but is only a physical reference to the sample's location within the curated core.

A full identification number for a sample consists of the following information: Leg, Site, Hole, Core Number, Core Type, Section Number, Piece Number (for hard rock), and Interval in centimeters measured from the top of section. For example, a sample identification of "124-768B-39R-3, 100–102 cm" would be interpreted as representing a sample removed from the interval between 100 and 102 cm below the top of Section 3, Core 39 (R indicates that this core was taken with the rotary core barrel) of Hole 768B during Leg 124.

All ODP core and sample identifiers indicate core type. The following abbreviations are used: R = rotary core barrel (RCB); H = hydraulic piston core (HPC; also referred to as APC, or advanced hydraulic piston core); P = pressure core barrel; X = extended core barrel (XCB); B = drill-bit recovery; C = center-bit recovery; I = *in-situ* water sample; S = sidewall sample; W = wash-core recovery; and M = miscellaneous material. APC, XCB, and RCB cores were cut on ODP Leg 124.

Core Handling

Sediments

As soon as a core is retrieved on deck, a sample is taken from the core catcher and given to the paleontological laboratory for an initial age assessment. The core is then placed on the long horizontal rack, and gas samples may be taken by piercing the core liner and withdrawing gas into a vacuum tube. Voids within the core are sought as sites for gas sampling. Some of the gas samples are stored for shore-based study, but others are analyzed immediately as part of the shipboard safety and pollution-prevention program. Next, the core is marked into section lengths, each section is labeled, and the core is cut into sections. Interstitial-water (IW) and organic geochemistry (OG) samples are then taken. In addition, some headspace gas samples are scraped from the ends of cut sections on the catwalk and sealed in glass vials for light hydrocarbon analysis. Each section is then sealed at the top and bottom by gluing on color-coded plastic caps, blue to identify the top of a section and clear for the bottom. A yellow cap is placed on section ends from which a whole-round sample has been removed. The caps are usually attached to the liner by coating the end liner and the inside rim of the cap with acetone, and taping the caps to the liners.

The cores then are carried into the laboratory, where the sections are again labeled, using an engraver to permanently mark the full designation of the section. The length of the core in each section and the core-catcher sample are measured to the nearest centimeter; this information is logged into the shipboard CORELOG database program.

Next, the whole-round sections from APC and XCB cores are run through the GRAPE (gamma-ray attenuation porosity evaluator) and *P*-wave logger devices to measure the bulk density, porosity, and sonic velocity. Magnetic susceptibility measurements follow. After the core has equilibrated to room temperature (this took approximately 2 to 4 hr on Leg 124), thermal conductivity measurements are made immediately before the cores are split.

Hydrocarbon Gases

For safety considerations gas concentrations were monitored in cores at 9-m intervals. Gases were extracted from bulk sediments utilizing headspace or vacutainer sampling techniques (Emeis and Kvenvolden, 1986). Vacutainer gas samples were taken immediately after core retrieval by piercing the core liner and withdrawing gas into a vacuum tube. Voids within the core are sought as sites for gas sampling by this technique. The headspace analyses were performed on about 5 g of sediment that was placed in a glass container sealed with a septum and metal crimp and then heated to 70°C for about 45 min. A 5-cm^3 sample of headspace gas was subsequently injected by means of a syringe into a gas chromatograph.

All headspace and Vacutainer gas samples were analyzed with a Carle AGC 1000/Model 211. This instrument was designed to measure accurately and rapidly the concentrations of methane, ethane, and propane using a flame ionization detector. The gas chromatograph (GC) was attached to a Hewlett-Packard Model 3393A integrator that allowed the direct measurement of gas concentrations after appropriate calibration. Occasionally, gases from aliquots of sediments or Vacutainer samples were also measured with a Hewlett-Packard 5890 natural gas analyzer (NGA) if the previous analysis revealed a significant propane concentration. This chromatograph is fitted with Porapak Q, molecular sieve and silicone oil-coated columns and both thermal conductivity (TCD) and flame ionization (FID) detectors. Gases measured with the NGA during Leg 124 include the suite of C_1–C_6 hydrocarbons. Generally, all gas concentrations are reported in ppm released from 5 g of wet sediment. The details of the configuration of the gas chromatographs are available in Emeis and Kvenvolden (1986).

Cores of relatively soft material are split lengthwise into working and archive halves. The softer cores are split with a wire or saw, depending on the degree of induration. Harder cores are split with a band saw or diamond saw. As cores on Leg

124 were split with wire from the bottom to top, older material could possibly have been transported up the core on the split face of each section. One should, therefore, be aware that the very near-surface part of the split core could be contaminated.

The working half is sampled for both shipboard and shore-based laboratory studies. Each extracted sample is logged in the sampling computer database program by the location and the name of the investigator receiving the sample. Records of all removed samples are kept by the curator at ODP. The extracted samples are sealed in plastic vials or bags and labeled. Samples are routinely taken for shipboard physical property analysis; these samples were subsequently used for calcium carbonate determinations (coulometric analysis). These data are reported in the site chapters.

The archive half is described visually. Smear slides are made from samples taken from the archive half and are supplemented by thin sections taken from the working half. Archive-half sections that show little drilling disturbance are run through the cryogenic magnetometer. The archive half is then photographed with both black-and-white and color film, a whole core at a time. Close-up black-and-white photographs are taken of particular features for illustrations in the summary of each site.

Both halves of the core are then put into labeled plastic tubes, sealed, and transferred to cold-storage space aboard the drilling vessel. At the end of the leg, the cores are transferred from the ship in refrigerated airfreight containers to cold storage at the Gulf Coast Repository at the Ocean Drilling Program, Texas A&M University, College Station, Texas.

Igneous Rocks

Igneous rock cores are handled differently from the sedimentary cores. Once on deck, the core-catcher is placed at the bottom of the core liner and total core recovery is calculated by shunting the rock pieces together and measuring to the nearest centimeter; this information is logged into the shipboard core-log database program. The core is then cut into 1.5-m-long sections and transferred into the lab. In some cases, magnetic susceptibility measurements were conducted on the whole-round cores before being split.

The contents of each section are transferred into 1.5 m-long sections of split core liner, where the bottom of oriented pieces (i.e., pieces that clearly could not have rotated top to bottom about a horizontal axis in the liner) are marked with a red wax pencil. This is to ensure that orientation is not lost during the splitting and labeling process. The core is then split into archive and working halves. A plastic spacer is used to separate individual pieces, and/or reconstructed groups of pieces, in the core liner. These spacers may represent a substantial interval of no recovery. Each piece is numbered sequentially from the top of each section, beginning with number 1; reconstructed groups of pieces are assigned the same number, but are lettered consecutively. Pieces are labeled on the rounded, not sawn surfaces. If the piece is oriented, an arrow is added to the label pointing to the top of the section.

The working half is sampled for shipboard laboratory studies. Records of all samples are kept by the curator at ODP. Minicore samples are routinely taken for physical properties and magnetic studies, some of which are later subdivided for XRF analysis and thin sectioning, so that as many measurements as possible are made on the same pieces of rock. At least one minicore is taken per lithological unit when recovery permits, generally from the freshest areas of core. Additional thin sections, X-ray diffraction (XRD) samples, and X-ray fluorescence (XRF) samples are selected from areas of particular interest. Samples for shore-based studies are selected in a sampling party held after drilling has terminated.

The archive half is described visually, then photographed with both black and white and color film, a core at a time. Both halves of the core are then shrink wrapped in plastic to prevent rock pieces from vibrating out of sequence during transit, put into labeled plastic tubes, sealed, and transferred to cold-storage space aboard the drilling vessel.

SEDIMENT CORE DESCRIPTION FORMS

The sediment core description forms (Fig. 3), or "barrel sheets," summarize the data obtained during shipboard analysis of each sediment core (see notes on igneous rock core description, below). The following discussion explains the ODP conventions used in compiling each part of the core description forms and the exceptions to these procedures adopted by Leg 124 scientists.

Core Designation

Cores are designated using leg, site, hole, core number, and core type as previously discussed (see "Numbering of Sites, Holes, Cores, and Samples" section, this chapter). In addition, the cored interval is specified in terms of meters below sea level (mbsl) and meters below seafloor (mbsf). On Leg 124, these depths were based on the drill-pipe measurements (DPM), as reported by the SEDCO coring technician and the ODP operations superintendent. The depths reported as mbsl were corrected for the height of the rig floor dual elevator stool above sea level (10.8–11.4 m during Leg 124) to yield true water depth.

Paleontological Data

Microfossil abundance, preservation, and zone assignment, as determined by the shipboard paleontologists, appear on the core-description form under the heading "Biostrat. Zone/Fossil Character." The chronostratigraphic unit, as recognized on the basis of paleontological results, is shown in the "Time-Rock Unit" column. Detailed information on the zonations and terms used to report abundance and preservation is presented in the "Biostratigraphy" section (this chapter).

Paleomagnetic, Physical Properties, and Chemical Data

Columns are provided on the core-description form to record paleomagnetic results, physical properties values (wet-bulk density, grain density, porosity, water content, and compressional velocity) and chemical data (percentages of $CaCO_3$ and total organic carbon determined using the Coulometrics analyzer and Rock-Eval pyrolysis, respectively). Additional information on shipboard procedures for collecting these types of data appears in the "Paleomagnetics," "Physical Properties," and "Inorganic Geochemistry" sections (this chapter).

Graphic Lithology Column

The lithological classification scheme of Mazzullo, Meyer, and Kidd (1987), accepted for shipboard use by the JOIDES Sediments and Ocean History Panel, was used in a slightly modified form on Leg 124. The classification adopted is outlined in a later section. Sediment type is represented graphically on the core description forms using the symbols illustrated in Figure 4.

Sediment Disturbance

In some cases the coring technique, which uses a 25-cm diameter bit with a 6-cm diameter core opening, may result in varying degrees of disturbance of the recovered core material. This is illustrated in the "Drilling Disturbance" column on the Core-Description Form (using the symbols in Fig. 5). The fol-

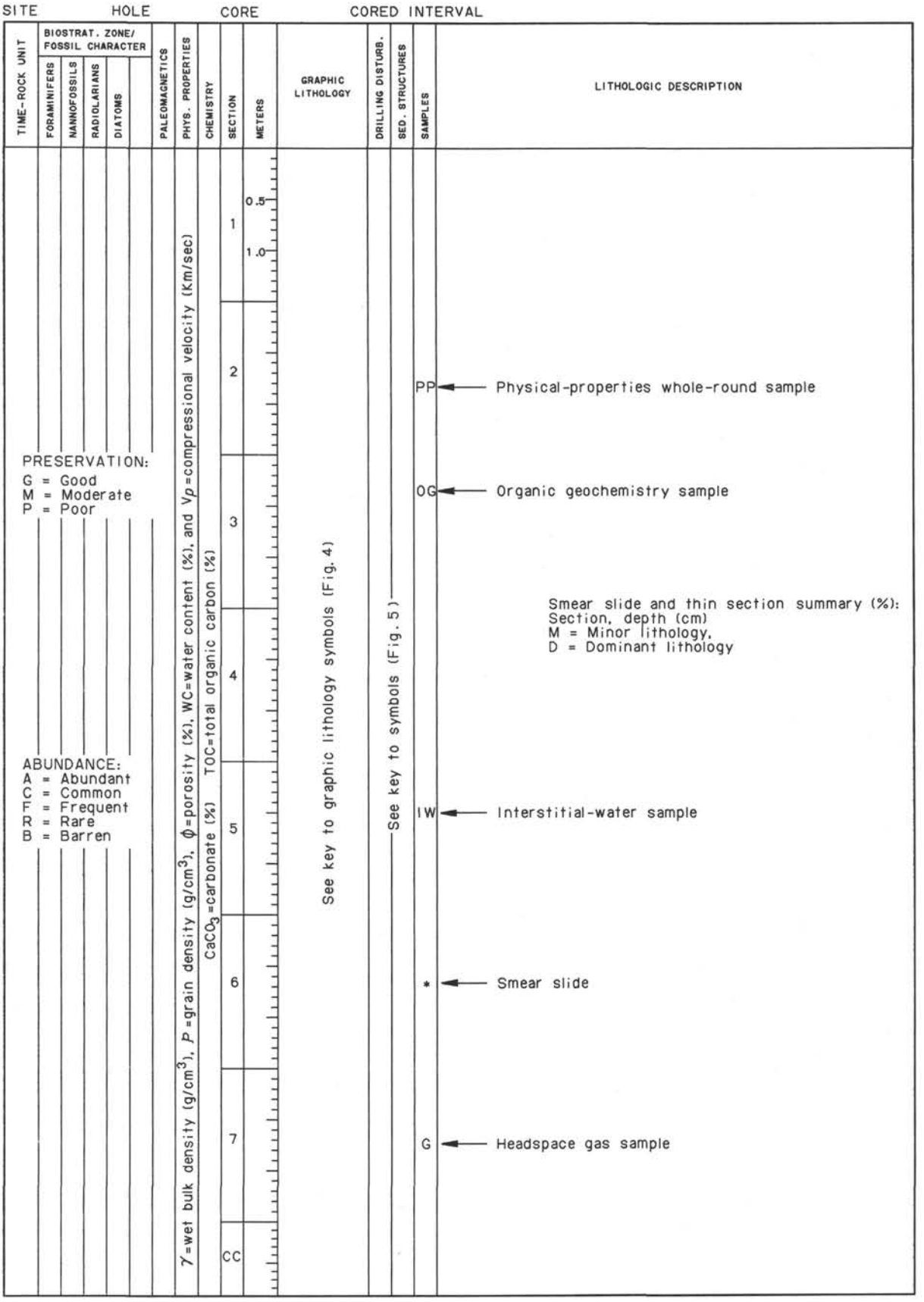

Figure 3. Core description form ("barrel sheet") used for sediments and sedimentary rocks.

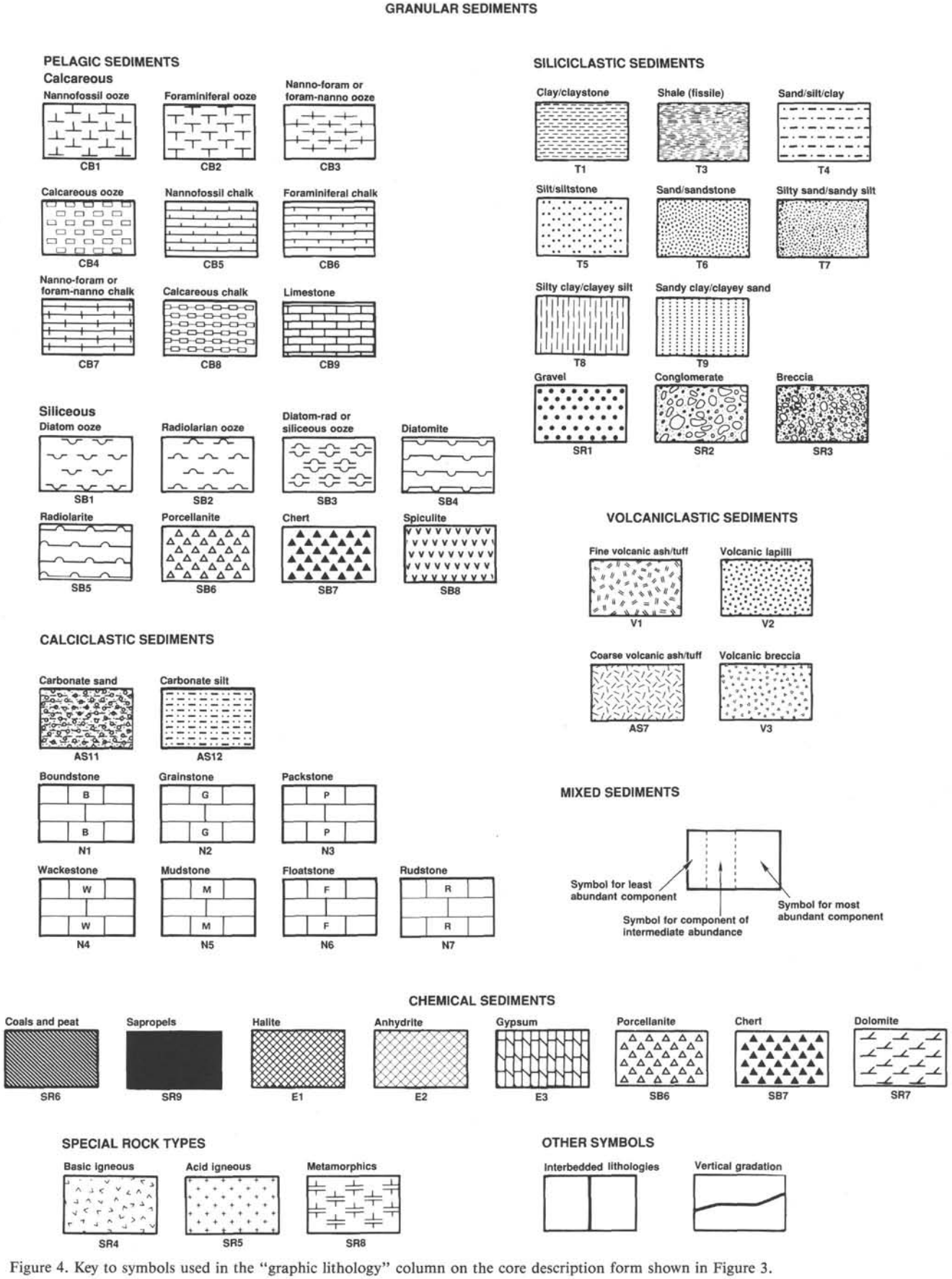

Figure 4. Key to symbols used in the "graphic lithology" column on the core description form shown in Figure 3.

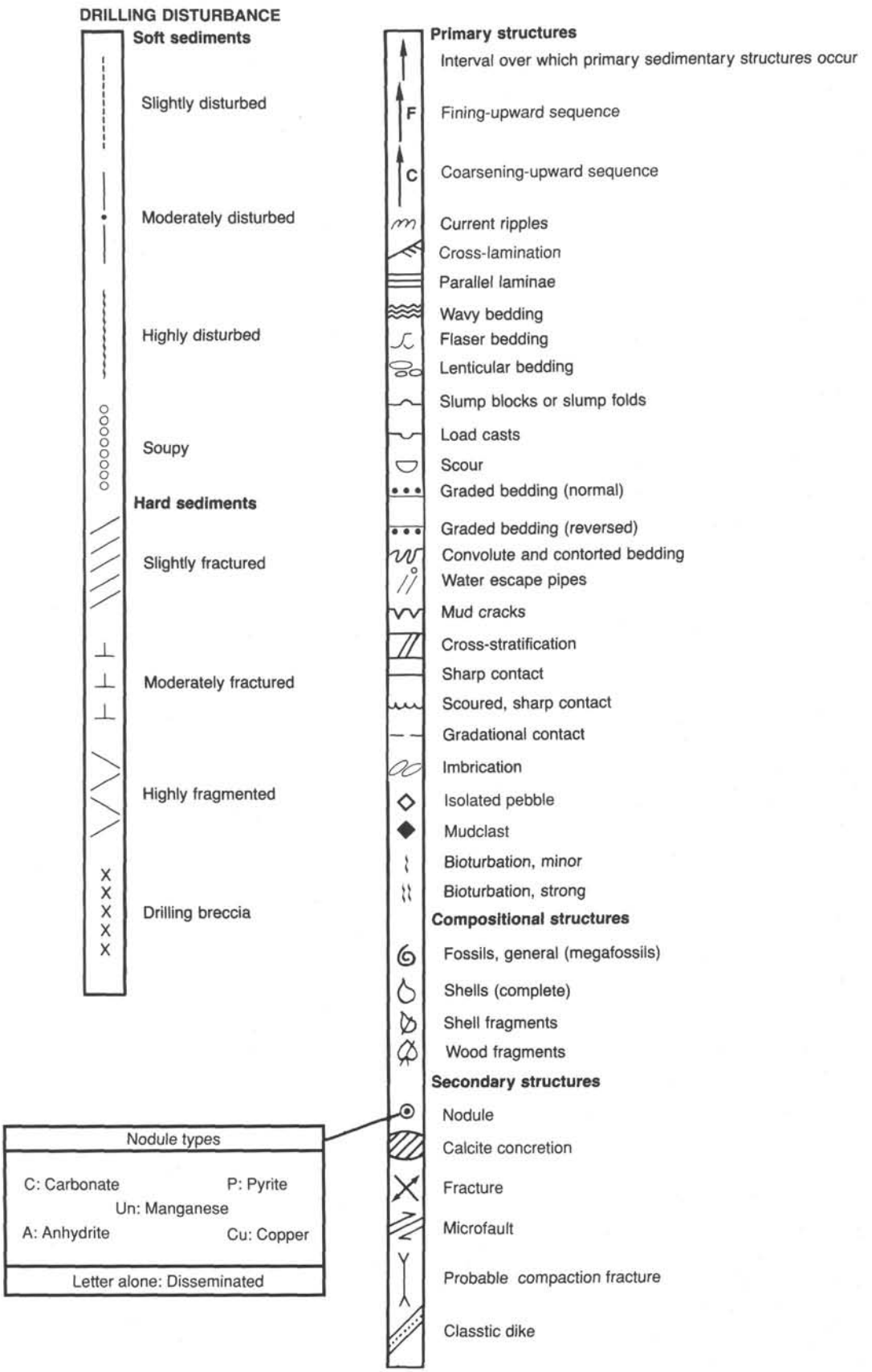

Figure 5. Symbols used for drilling disturbance and sedimentary structure on core description forms shown in Figure 3.

lowing disturbance categories are recognized for soft and firm sediments:

1. Slightly deformed: Bedding contacts are slightly bent.
2. Moderately deformed: Bedding contacts have undergone extreme bowing.
3. Highly deformed: Bedding is completely disturbed, sometimes showing symmetrical diapir-like structures ("flow-in").
4. Soupy: Intervals are water-saturated and have lost all aspects of original bedding.

The following categories are used to describe the degree of fracturing in hard sediments and igneous and metamorphic rocks (Fig. 5):

1. Slightly fractured: Core pieces are in place and have very little drilling slurry or breccia.
2. Moderately fragmented: Core pieces are in place or partly displaced, but original orientation is preserved or recognizable. Drilling slurry may surround fragments.
3. Highly fragmented: Pieces are from the interval cored and probably in correct stratigraphic sequence (although they may not represent the entire section), but original orientation is totally lost.
4. Drilling breccia: Core pieces have completely lost their original orientation and stratigraphic position and may be completely mixed with drilling slurry.

Sedimentary Structures

Observed sedimentary structures, including fining-upward and coarsening-upward sequences through series of beds, are indicated in the "Sedimentary Structure" column of the core description forms. A key to the symbols used on Leg 124 is given in Figure 5. Original sedimentary structures may have been destroyed in cores that have been severely disturbed by drilling.

Color

Colors of sediment are determined by comparison with the Geological Society of America Rock-Color Chart (Munsell Soil Color Chart, 1975). Colors were determined immediately after the cores were split and while they were still wet. Hard rocks were wetted before their color was determined.

Samples

The position of samples taken from each core for shipboard analysis is indicated in the "Samples" column in the Core Description Form. An asterisk (*) indicates the location of smear-slide samples. A number sign (#) indicates the location of thin sections, except for thin sections of igneous rock clasts, which are indicated by an open circle (o). The symbols IW and OG designate whole-round interstitial-water and frozen organic geochemistry samples, respectively.

Sample positions for physical property measurements are indicated by a circled dot in the "Physical Props." column, accompanied by the following symbols: γ = wet-bulk density (g/cm^3); ρ = grain density (g/cm^3); ϕ = porosity (%); wc = water content (%), and V_p = compressional velocity (km/s). Sample positions for routine geochemical analyses are indicated in the "Geochemistry" column: a dot labeled $CaCO_3$ denotes an inorganic carbon (%$CaCO_3$) analysis, and an asterisk (*) with the label TOC indicates analysis of total organic carbon (%TOC).

Paleomagnetic results (normal and reversed-polarity intervals) are indicated in the "Paleomagnetics" column.

Shipboard paleontologists generally base their age determinations on core-catcher samples, although additional samples from other parts of the core may be examined when required. The sample locations are shown in the appropriate column by letter codes indicating the abundance and preservation of the fossils. Examination of such samples may lead to the recognition of zonal boundaries in the core; these are also indicated in the appropriate column.

Lithologic Description—Text

The lithologic description that appears on each Core Description Form consists of brief summaries of the major lithologies observed, followed by a summary of the minor lithologies. The sedimentary structures, color, and composition of each lithology is described and, where appropriate, their distribution in the core. The thickness of sedimentary beds and laminae is described using the terminology of McKee and Weir (1953), which is outlined in Table 1. In cases where there are thin or very thin beds of a minor lithology, a description including occurrence information is included in the text, but the beds may be too thin (< 10 cm) to appear in the graphic lithology column.

Smear-Slide and Thin-Section Summary

A table summarizing the available smear-slide and thin-section data appears on each Sediment Core Description Form. The section and interval from which the sample was taken are noted (section, depth (cm)) as well as identification as a major "dominant" (D), or minor (M), lithology in the core. The percentages of sand, silt, and clay grain sizes and of all identified components is indicated. Trace amounts of components are indicated by "Tr." As explained in the following "Sediment Classification" section (this chapter), these data are used to classify the recovered material.

SEDIMENTOLOGY

The new classification scheme for the Ocean Drilling Program, by Mazzullo, Meyer, and Kidd (1987), partly reproduced below, was used in a modified form during Leg 124. The following are the major modifications adopted for Leg 124.

1. The term "neritic," used in the ODP classification for granular calcareous sediment of non-pelagic origin, is replaced by "calciclastic," following the terminology adopted on ODP Leg 119. In conventional usage the term "neritic" refers to the shelf depth zone (Bates and Jackson, 1980), and its use to refer to a descriptive sediment class may cause misunderstanding. The "calciclastic" sediment encountered during Leg 124 is primarily reworked and redeposited carbonate sediment derived from shelf to bathyal depths, which is interbedded with pelagic and hemipelagic sediment deposited at bathyal to abyssal depths.

2. In the ODP classification, "neritic" sediments are described using the terminology of Dunham (1962), which is based on texture and fabric. While use of this classification for indurated limestones is well established, its application to unlithified carbonate sediments is unsatisfactory. Rock names in the Dunham scheme (such as "packstone" and "wackestone") carry an inherent connotation of induration. Furthermore, the major means of shipboard microscopic examination of unlithified sediments (smear-slide analysis) is fabric-destructive, making correct application of the classification difficult. In naming unlithified

Table 1. Bed thickness terminology used in lithologic description of cores (McKee and Weir, 1953).

Thickness term	Range (cm)
Very thick bedded	>100
Thick bedded	30–100
Medium bedded	10–30
Thin bedded	3–10
Very thin bedded	1–3
Thickly laminated	0.3–1
Thinly laminated	<0.3

"calciclastic" sediment on Leg 124, we have used a scheme based on grain size, which is outlined below.

3. Mixed sediments composed of 40 to 60% pelagic carbonate and 40 to 60% clay and silt-sized siliciclastic and volcaniclastic grains are termed "marl" ("marlstone" if the sediment is lithified) in the sediment descriptions for Leg 124. These terms were added to the nomenclature to avoid the repeated use of cumbersome sediment names: for example, "clayey nannofossil mixed sediment" (full ODP classification) is reduced to "nannofossil marl" (Leg 124 amendment).

4. Fine-grained volcaniclastic sediments have been divided into two size classes. Unlithified volcaniclastic material 1/16 to 2 mm in grain size (equivalent to sand in siliciclastic sediments) is described as "coarse ash," and material less than 1/16 mm (silt and clay-size) is termed "fine ash." "Coarse tuff" and "fine tuff" are the terms used for lithified equivalents of these size ranges.

The sediment classification scheme described here defines two basic sediment types: (1) granular sediments and (2) chemical sediments.

Granular Sediments

Classes of Granular Sediments

Four types of grain are recognized in granular sediments: pelagic, calciclastic, siliciclastic, and volcaniclastic. Pelagic grains are composed of the fine-grained skeletal debris of open-marine siliceous and calcareous microfauna and microflora (e.g., radiolarians, nannofossils) and associated organisms. Calciclastic grains are composed of coarse-grained calcareous skeletal debris (e.g., bioclasts, peloids), and fine-grained calcareous grains of nonpelagic origin. Siliciclastic grains are composed of mineral and rock fragments that were derived from plutonic, sedimentary, and metamorphic rocks. Volcaniclastic grains are composed of rock fragments and minerals that were derived from volcanic sources.

Variations in the relative proportions of these four grain types define five major classes of granular sediments: pelagic, calciclastic, siliciclastic, volcaniclastic, and mixed (Fig. 6).

Pelagic sediments are composed of more than 60% pelagic and calciclastic grains and less than 40% siliciclastic and volcaniclastic grains, and contain a higher proportion of pelagic than calciclastic grains.

Calciclastic sediments are composed of more than 60% pelagic and calciclastic grains and less than 40% siliciclastic and volcaniclastic grains, and contain a higher proportion of calciclastic than pelagic grains.

Siliciclastic sediments are composed of more than 60% siliciclastic and volcaniclastic grains and less than 40% pelagic and calciclastic grains, and contain a higher proportion of siliciclastic than volcaniclastic grains.

Volcaniclastic sediments are composed of more than 60% siliciclastic and volcaniclastic grains and less than 40% pelagic and calciclastic grains, and contain a higher proportion of volcaniclastic than siliciclastic grains. This class includes epiclastic sediments (volcanic detritus that is produced by erosion of volcanic rocks by wind, water, and ice), pyroclastic sediments (the products of the degassing of magmas), and hydroclastic sediments (the products of the granulation of volcanic glass by steam explosions).

Lastly, mixed sediments are composed of 40%–60% siliciclastic and volcaniclastic grains, and 40%–60% pelagic and neritic grains. The term "marl" describes the specific type of mixed sediments in which the pelagic fraction is mostly biogenic carbonate.

Classification of Granular Sediment

A granular sediment can be classified by designating a principal name and major and minor modifiers. The principal name of a granular sediment defines its granular-sediment class; the major and minor modifiers describe the texture, composition, fabric, and/or roundness of the grains themselves (Table 2).

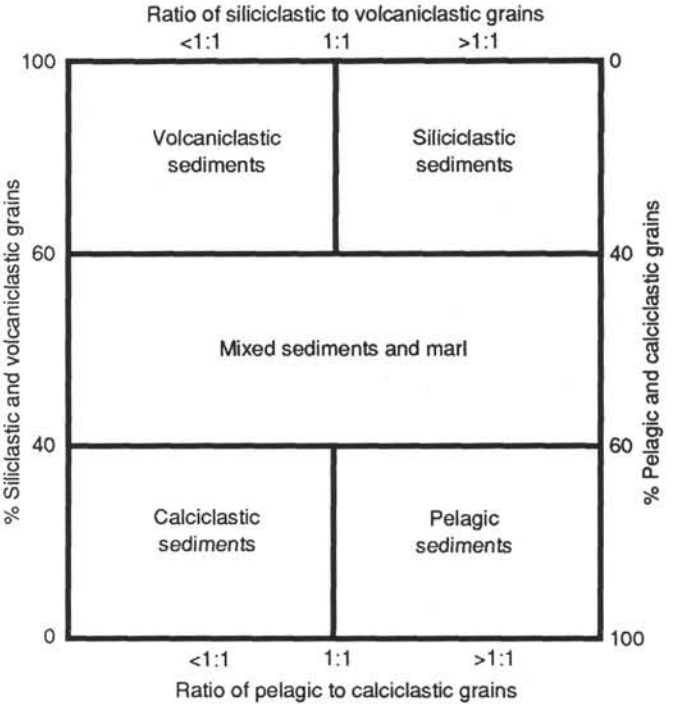

Figure 6. Diagram showing classes of granular sediment (modified from Mazzullo et al., 1987). The term "marl" is used to indicate mixed sediments composed of 40%–60% pelagic carbonate and 40%–60% clay and silt-sized siliciclastic and volcaniclastic grains.

Principal Names

Each granular-sediment class has a unique set of principal names, which are outlined as follows.

For pelagic sediment, the principal name describes the composition and degree of consolidation using the following terms:

1. Ooze: Unconsolidated calcareous and/or siliceous pelagic sediments;
2. Chalk: Firm pelagic sediment composed predominantly of calcareous pelagic grains;
3. Limestone: Hard pelagic sediment composed predominantly of calcareous pelagic grains;
4. Radiolarite, diatomite, and spiculite: Firm pelagic sediment composed predominantly of siliceous radiolarians, diatoms, and sponge spicules, respectively; and
5. Chert: Hard pelagic sediment composed predominantly of siliceous pelagic grains.

For unlithified calciclastic sediment, the principal name describes the texture (grain size), using the following terms:

1. Carbonate sand: Soft calciclastic sediment with grain size between 1/16 mm and 2 mm;
2. Carbonate silt: Soft calciclastic sediment with grain size between 1/256 mm and 1/16 mm; and
3. Micrite: Soft, clay-sized calciclastic sediment (grain size $<1/256$ mm).

For lithified calciclastic sediment, the principal name describes the texture and fabric, using the following terms (from Dunham, 1962):

1. Boundstone: Components organically bound during deposition;
2. Grainstone: Grain-supported fabric, no mud, grains <2 mm in size;

Table 2. Outline of granular-sediment classification scheme (modified from Mazzullo et al., 1987).

Sediment class	Major modifiers	Principal names	Minor modifiers
Pelagic Sediment	1. composition of pelagic and calciclastic grains present in major amounts 2. texture of clastic grains present in major amounts	1. ooze 2. chalk 3. limestone 4. radiolarite 5. diatomite 6. spiculite 7. chert	1. composition of pelagic and calciclastic grains present in minor amounts 2. texture of clastic grains present in minor amounts
Calciclastic Sediment	1. composition of calciclastic and pelagic grains present in major amounts 2. texture of clastic grains present in major amounts	1. boundstone 2. grainstone 3. packstone 4. wackestone 5. mudstone 6. floatstone 7. rudstone	1. composition of calciclastic and pelagic grains present in minor amounts 2. texture of clastic grains present in minor amounts
Siliciclastic Sediment	1. composition of all grains present in major amounts 2. grain fabric (gravels only) 3. grain shape (optional) 4. sediment color (optional)	1. gravel 2. sand 3. silt 4. clay (etc.)	1. composition of all grains present in minor amounts 2. texture and composition of siliciclastic grains present as matrix (for coarse-grained clastic sediments)
Volcaniclastic Sediment	1. composition of all volcaniclasts present in major amounts 2. composition of all pelagic and calciclastic grains present in major amounts 3. texture of siliciclastic grains present in major amounts	1. breccia 2. lapilli 3. coarse ash/tuff 4. fine ash/tuff	1. composition of all volcaniclasts present in minor amounts 2. composition of all calciclastic and pelagic grains present in minor amounts 3. texture of siliciclastic grains present in minor amounts
Mixed Sediment	1. composition of calciclastic and pelagic grains present in major amounts 2. texture of clastic grains present in major amounts	1. mixed sediments 2. marl/marlstone	1. composition of calciclastic and pelagic grains present in minor amounts 2. texture of clastic grains present in minor amounts

3. Packstone: grain-supported fabric, with intergranular mud, grains <2 mm in size;
4. Wackestone: Mud-supported fabric, with greater than 10% grains, grains <2 mm in size;
5. Mudstone: Mud-supported fabric, with less than 10% grains;
6. Floatstone: Matrix-supported fabric, grains >2 mm in size; and
7. Rudstone: Grain-supported fabric, grains >2 mm in size.

For siliciclastic sediment, the principal name describes the texture and is assigned according to the following guidelines:

1. The Udden-Wentworth grain-size scale (Wentworth, 1922; Table 3) defines the grain-size ranges and the names of the textural groups (gravel, sand, silt and clay) and sub-groups (fine sand, coarse silt, etc.) that are used as the principal names of siliciclastic sediment.
2. When two or more textural groups or sub-groups are present in a siliciclastic sediment, they are listed as principal names in order of increasing abundance (Shepard, 1954; Fig. 7).
3. The suffix"-stone" can be affixed to the principal names sand, silt, and clay when the sediment is lithified; shale can be used as a principal name for a lithified and fissile siltstone or claystone. Conglomerate and breccia are used as principal names of gravels with well-rounded and angular clasts, respectively.

For volcaniclastic sediment, the principal name describes the texture. The names and ranges of three textural groups (from Fisher and Schmincke, 1984) are as follows:

1. Volcanic breccia: Pyroclasts greater than 64 mm in diameter;
2. Volcanic lapilli: Pyroclasts between 2 and 64 mm in diameter; when lithified, use the name lapillistone; and
3. Volcanic ash: Pyroclasts less than 2 mm in diameter; when lithified, use the name tuff. For Leg 124, this group was subdivided into two classes by grain size: coarse ash/tuff, with grains between 1/16 and 2 mm in size, and fine ash/tuff, with grains <1/16 mm in size.

For mixed sediment, the principal name describes the degree of consolidation, using the terms mixed sediments or mixed sedimentary rocks. Mixed sediments composed of 40%–60% pelagic carbonate and 40%–60% clay and silt-sized siliciclastic and volcaniclastic grains are termed "marl" ("marlstone" if the sediment is lithified) in the sediment descriptions for Leg 124.

Major and Minor Modifiers

The principal name of a granular-sediment class is preceded by major modifiers and followed by minor modifiers (preceded by the suffix "with") that describe the lithology of the granular sediment in greater detail (Table 2). The most common uses of major and minor modifiers are to describe the composition and textures of grain types that are present in major (>25%) and minor (10%–25%) proportions. In addition, major modifiers can be used to describe grain fabric, grain shape, and sediment color. The nomenclature for the major and minor modifiers is outlined as follows:

The composition of pelagic grains can be described with the major and minor modifiers diatom(-aceous), radiolarian, spicules(-ar), siliceous, nannofossil, foraminifer, and calcareous. The terms siliceous and calcareous are used generally to describe sediments that are composed of siliceous or calcareous pelagic grains of uncertain origins.

Table 3. Udden-Wentworth grain-size scale for siliclastic sediments (Wentworth, 1922).

Millimeters	Microns	Phi (ϕ)	Wentworth size class	
		−20		
4096		−12	Boulder (−8 to −12ϕ)	
1024		−10		
256		−8	Cobble (−6 to −8ϕ)	Gravel
64		−6		
16		−4	Pebble (−2 to −6ϕ)	
4		−2		
3.36		−1.75		
2.83		−1.5	Granule	
2.38		−1.25		
2.00		−1.0		
1.68		−0.75		
1.41		−0.5	Very coarse sand	
1.19		−0.25		
1.00		0.0		
0.84		0.25		
0.71		0.5	Coarse sand	
0.59		0.75		
1/2 — 0.50	500	1.0		
0.42	420	1.25		
0.35	350	1.5	Medium sand	Sand
0.30	300	1.75		
1/4 — 0.25	250	2.0		
0.210	210	2.25		
0.177	177	2.5	Fine sand	
0.149	149	2.75		
1/8 — 0.125	125	3.0		
0.105	105	3.25		
0.088	88	3.5	Very fine sand	
0.074	74	3.75		
1/16 — 0.0625	63	4.0		
0.053	53	4.25		
0.044	44	4.5	Coarse silt	
0.037	37	4.75		
1/32 — 0.031	31	5.0		Mud
1/64 0.0156	15.6	6.0	Medium silt	
1/128 0.0078	7.8	7.0	Fine silt	
1/256 — 0.0039	3.9	8.0	Very fine silt	
0.0020	2.0	9.0		
0.00098	0.98	10.0		
0.00049	0.49	11.0	Clay	
0.00024	0.24	12.0		
0.00012	0.12	13.0		
0.00006	0.06	14.0		

The composition of calciclastic grains can be described with the following major and minor modifiers:

1. Ooid (or oolite): spherical or elliptical non-skeletal particles smaller than 2 mm in diameter, having a central nucleus surrounded by a rim with concentric or radial fabric;
2. Bioclast (or bioclastite): fragment of skeletal remains. Specific names such as molluscan or algal can also be used;
3. Pellet (-al): Fecal particles from deposit-feeding organisms;
4. Intraclast: Reworked carbonate-rock fragment or rip-up clast;
5. Pisolite: Spherical or ellipsoidal non-skeletal particle, commonly greater than 2 mm in diameter, with or without a central nucleus but displaying multiple concentric layers of carbonate;
6. Peloid (pel): Micritized carbonate particle of unknown origin; and
7. Calcareous, dolomitic, aragonitic, sideritic: these modifiers should be used to describe the composition of carbonate muds or mudstones (micrite) of non-pelagic origins.

The texture of siliciclastic grains is described by the major and minor modifiers gravel(-ly), sand(-y), silt(-y), and clay(-ey). The composition of siliciclastic grains can be described by:

1. Mineralogy: using modifiers such as "quartz," "feldspar," "glauconite," "mica," "kaolinite," "zeolitic," "lithic" (for rock fragments), "calcareous," "gypsiferous," or "sapropelic" (for detrital clasts of calcium carbonate, gypsum, and organic matter, respectively); and
2. Provenance: The source of rock fragments (particularly in gravels, conglomerates, and breccias) can be described by modifiers such as volcanic, sed-lithic, meta-lithic, gneissic, basaltic, etc.

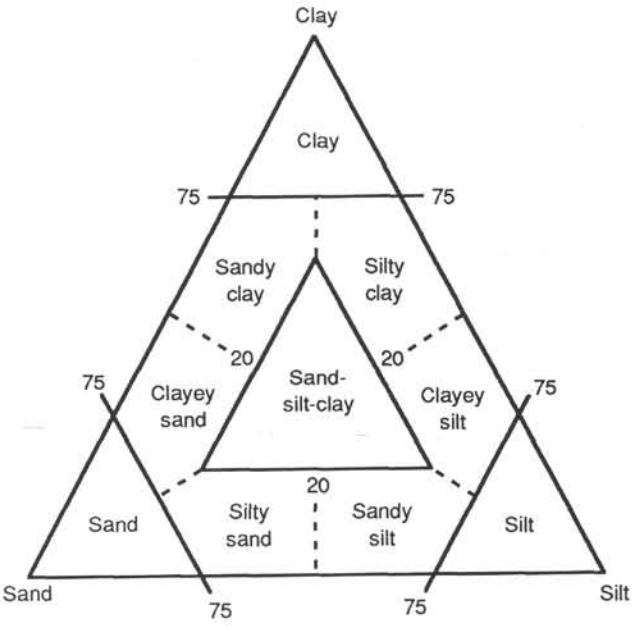

Figure 7. Ternary diagram showing principal names for siliciclastic sediments (from Shepard, 1954).

The composition of volcaniclastic grains is described by the major and minor modifiers lithic (rock fragments), vitric (glass and pumice), and crystal (mineral crystals), or by modifiers that describe the compositions of the lithic grains and crystals (e.g., feldspar or basaltic). The fabric of the sediment can be described by the major modifiers grain-supported, matrix-supported, and imbricated. Generally, fabric descriptors are applied only to gravels, conglomerates, and breccias, for they provide useful information on their transport history.

The shapes of grains are described by the major modifiers rounded, sub-rounded, sub-angular, and angular.

The color of sediment is determined with a standard color-comparitor, such as the Munsell Chart, and can be employed as a major modifier.

Chemical Sediments

Classes of Chemical Sediment

Chemical sediment is composed of minerals that formed by inorganic processes such as precipitation from solution or colloidal suspension, deposition of insoluble precipitates, or recrystallization of detrital evaporites and siliceous, calcareous, or carbonaceous (plant) biogenic debris, and generally has a crystalline (i.e., non-granular) texture.

There are five classes of chemical sediments: Carbonaceous sediments, evaporites, silicates, carbonates, and metalliferous sediments. Each class of chemical sediment has its own distinctive classification scheme.

Carbonaceous Sediments

Carbonaceous sediments are composed of greater than 50% organic remains, principally plant and algal, that have been altered by carbonization, bituminization, or putrification from

their original form. The two most common varieties of carbonaceous sediments are the coal series and sapropels.

The coal series is classified according to rank. Four ranks are recognized and used as principal names:

1. Peat: Soft, earthy organic debris with recognizable plant fragments;
2. Brown coal: Few recognizable plant fragments, but the coal is soft, dull, and brown;
3. Bituminous coal: Black and hard with bright layers, and breaks into cuboidal fragments along cleats; and
4. Anthracite coal: bright and lustrous, with conchoidal fractures.

The principal name of the coal series can be modified by terms that describe non-carbonaceous components such as clastic detritus (e.g., muddy peat).

Evaporites

Evaporites are composed of minerals produced from a saline solution that became concentrated by evaporation of the solvent. The evaporites are classified according to their mineralogy using terms such as halite, gypsum, and anhydrite. They may be modified by terms that describe their structure or fabric, such as massive, nodular, nodular-mosaic and chicken wire.

Silicates/Carbonates

Silicates and carbonates are defined as sedimentary rocks that are non-granular and non-biogenic in appearance and composed of silicate and carbonate minerals. Silicates and carbonates may have formed from the recrystallization of siliceous and calcareous grains, but are distinguished by the absence of clearly identifiable granular and biogenic components. They may also form as primary precipitates, as in the case of dolomite or proto-dolomite, or as hydrothermal alteration products such as in the case of zeolites. They are classified according to their mineralogy, using principal names such as chert (microcrystalline quartz), calcite, and dolomite. They should also be modified with terms which describe their crystalline (as opposed to granular) nature, such as crystalline, microcrystalline, massive, and amorphous.

Metalliferous Sediments

Metalliferous sediments are a broad category of non-granular, non-biogenic sedimentary rocks that include pyrite, goethite, manganese, chamosite, glauconite, and other metal-bearing minerals. They are classified according to their mineralogy.

Grain-Size Measurements

For routine assignment of sediments to textural classes, grain sizes were estimated visually from the core material and smear slides. To supplement these determinations of grain size, a Lasentec Lab-Tec 100 particle-size analyzer was used on samples in the upper part of Hole 767B on Leg 124. This instrument uses the scattering of light from a laser source by particles in suspension to determine the distribution of grain sizes. The procedures outlined here were followed.

1. Sample preparation: A small quantity of sediment was placed in one of the beakers designed for use with the Lab-Tec 100, and about 25 cm^3 of 1% Calgon solution plus 75 cm^3 of water added. If the sample was clearly rich in clay, the beaker was placed in an ultrasonic bath for 2–3 min (as suggested in the LASENTEC manual). The beaker was then placed in the particle-size analyzer and mixed by the magnetic stirrer for 2–3 min before measurements were started.

2. Setting up the particle-size analyzer: The instructions in section 2.3 of the LASENTEC manual were followed. Range 'C' (<2 to >125 μm) on the dial at the back of the control unit was selected. A count time of 1.5 s was generally used. (The count time may need to be reduced if the sediment is too concentrated or increased if the dispersion is very fine—see section 2.3.1 of the LASENTEC manual.) Fine tuning of the focus did not seem to have any significant effect on the results in a number of test runs using the instrument: a micrometer reading of 2.5 mm was used for all analyses. Compensation factors of 1 were used for all size ranges (see below).

3. Operation: Once the sediment was adequately suspended by the stirrer, the operation instructions (Section 3 of the LASENTEC manual) were followed. A "true average" output was selected, and the count continued until the percentage for each size was static (5–10 count cycles). The data were then output to the printer.

Comments on the Use of the LASENTEC LAB-TEC 100 Particle-size Analyzer

Grain-size determination by smear-slide examination is necessarily subjective, and the LAB-TEC 100 offers an objective means of assessing particle-size distribution in a sediment. However, we feel that there are a number of questions and problems to be resolved if this instrument is to be used in routine grain-size analysis.

Compensation Factors

The scattering effect is determined by the surface area of the particles in suspension; hence the instrument determines the abundance of grains in each size class according to their *surface areas*. However, in normal practice sediments are classified according to the *weight percentage* in different size classes. To convert the measured abundances to weight percentage, it is necessary to multiply the value for each grain-size class by a compensation factor. This presents a number of problems. First, the appropriate compensation factors do not seem to have been established, and would vary with different sediment compositions. Second, the raw uncompensated results (expressed as surface area abundances) are more directly comparable with smear-slide determination than weight percentages. Third, empirical assessment of grain sizes by the "feel" and "grittiness" of sediments indicated that the uncompensated results are a better assessment of the grain-size distribution.

Coarse Sediments

Analyses of sediments containing sand-size particles yielded results that clearly underestimated the proportion of sand-size material. Underestimation occurs because the coarser material is more difficult to maintain in suspension and does not reach the level of the focused laser beam.

Fine Sediments

Analyses of clayey sediments in Hole 767B clearly underestimated the proportion of the clay size class. This effect is attributed to incomplete disaggregation of the sediment; much of the clay remains as flocculated aggregates that register as silt-size grains. This problem becomes more acute with increasing depth in the section as the degree of lithification and difficulty in disaggregating the sample increase. A number of samples were subjected to more thorough disaggregation by agitation in calgon deflocculant for 24 hr before grain-size analyses were made. These results were not significantly different from those obtained after shorter sample preparation periods.

It is suggested that the LASENTEC Lab-Tec 100 particle-size analyzer is only suitable for totally unlithified sediments in the highest parts of a hole, provided that these sediments do not contain any material coarser than silt. The results obtained would still need to be related to conventional grain-size distributions using compensation factors that have yet to be determined for different sediments.

X-ray Diffraction (XRD) Analysis

A Philips ADP 3520 X-ray diffractometer was used for the X-ray diffraction (XRD) analysis of clay minerals. Instrument conditions were as follows:

CuK-alpha radiation with a Ni filter
Tube voltage 40 kV
Tube current 35 mA

Samples were scanned from 2° to 15° (2θ) in 0.02° by 1-s steps in both unglycolated and glycolated states and from 24° to 26° (2θ) in 0.005° by 1-s steps in the glycolated state only.

Samples were placed in 50 mL polyethylene centrifuge tubes and disaggregated after soaking overnight in buffered acetic acid solution (1 M sodium acetate buffered to pH = 5.0) warmed in a beaker of water on a hot plate. Disaggregation was generally assisted by stirring with a glass rod. This treatment also removed calcium carbonate. Samples were then centrifuged at 1500 for 15 min, the supernate discarded and resuspended in a 1% solution of sodium hexametaphosphate (Calgon) to deflocculate the clays. The samples were centrifuged again at 1500 rpm for 15 min. This treatment was repeated as necessary to obtain an unflocculated sample.

Samples were then resuspended in 1% Calgon and centrifuged for 5 min at 1000 rpm to remove the size fraction greater than 2 μm in effective settling diameter. The supernate was decanted into another 50-mL centrifuge tube and centrifuged at 1500 rpm for 15 min to collect the size fraction less than 2 μm in diameter. In some samples a modest fraction of the sample remained in suspension and was discarded with the supernate.

The samples were then suspended in 5 to 10 mL of 1 M magnesium chloride solution and heated in a beaker of water on the hot plate for 1 hr to saturate exchangeable sites with magnesium. The treated samples were then centrifuged at 1500 rpm for 5 min, the supernate discarded, and washed with 10 mL of reverse osmosis (RO) water. These samples were centrifuged again at 1500 rpm for 5 min and the supernate discarded. Samples were then ready for mounting.

Samples were mounted on glass slides cut to fit in the Philips automatic sample changer sample holders. Mounts were made by stirring the sediment in the centrifuge tube with a spatula, placing a drop of the suspension on the slide and smearing with a clean glass microscope slide. Most samples were thick enough to be opaque; thin, semi-transparent mounts gave inferior results and were only used when sample volumes were very small.

Mounted samples were generally loaded directly into the Philips sample changer cassette and dried in the oven at 80°C. After drying and cooling to room temperature, samples were X-rayed as described above for unglycolated samples.

Upon completion, sample holders were removed from the cassette and placed in the glycolator. The glycolator consists of a metal desiccator containing approximately 100 mL of ethylene glycol beneath a perforated metal plate. The glycolator was then placed in the oven at 80°C for at least 90 min. Glycolated samples were then analyzed as described above. Whenever the 2° to 15° (2θ) measurement would not be completed within 6 hr of removal from the glycolator, samples were kept in the glycolator and re-glycolated immediately before measurement.

Data were provided both as tables and as plots of the entire scan. Data reduction was carried out on the plot of the glycolated run. Peak areas were approximated by multiplying the peak height times the "full width at half maximum" (FWHM). A straight-line background was drawn in and the peak height measured. A straight line, parallel to the background line, was drawn at one half the peak height. Vertical lines were drawn through the intersections of this half maximum line with the peak outline and the distance between measured parallel to the x-axis of the plot. This defined the FWHM. It is worth noting that the FWHM does not scale with the peak height and that the areas measured in this way at low peak intensities may be somewhat over estimated.

To calculate relative abundances, peak areas were weighted using the weights established by Biscaye (1965): 1x for the 17-Å smectite peak, 4x for the 10-Å illite peak, and 2x for the 7-Å kaolinite + chlorite peak. The weighted areas were summed and the individual weighted areas normalized. The area of the 7-Å peak was partitioned between kaolinite and chlorite using the peak heights of the 3.58-Å kaolinite and the 3.54- to 3.52-Å chlorite peaks. A straight-line background was constructed under these peaks and the peak shapes were reconstructed as either single or double triangles that reproduced the shape of the left side of the kaolinite peak under the chlorite peak and *vice versa* to correct for overlap. Results are reported as weight percent of the total of diffracting clays, and the abundances of smectite, illite, kaolinite, and chlorite reported here sum to 100%. Clays are reported as smectite, illite, kaolinite, and chlorite with no attempt to separate such polymorphs as celadonite, nontronite, saponite, etc., or to investigate the occurrence and/or abundance of mixed-layer clays.

The results of these analyses must be considered as subquantitative. Some error is induced by the method of calculating peak areas, some by the simple weighting factors used, some is especially induced in the kaolinite/chlorite determination by the relatively imprecise method of separating these species, and a considerable error may be due to intrinsic variations in the diffracting power of clays of varying grain sizes, crystallinity, and composition. With this *caveat* in mind, however, much useful information on the provenance of sedimentary clay minerals may be obtained by these methods.

X-ray Fluorescence (XRF) Analysis

The routine major-element analysis of sediments from Sites 767, 768, and 769 was carried out on pressed pellets to permit the analysis of sediments from every core recovered at these sites. Samples were dried at 110°C for at least 2 hr, then ground. Five grams of the resulting powder were mixed with 30 drops of polyvinyl alcohol binder and pressed at 7 tons into an aluminum cap. These pellets have been reserved for post-cruise trace-element analysis.

The fully automated ARL 8420 wavelength-dispersive X-ray fluorescence system was calibrated using between seven and ten standards for each element. An element standard and a drift standard were included with every six samples analyzed. Results are reported as the weight percentage of SiO_2, TiO_2, Al_2O_3, Fe_2O_3, MnO, MgO, CaO, Na_2O, K_2O, P_2O_5, and the sum of these oxide concentrations. Certain errors are inherent in this technique. The most common of these is that calcium is frequently present in sediments as $CaCO_3$, rather than CaO. The result is that many analyses do not approach 100% for the sum of their oxide concentrations and that there is a very strong inverse correlation between CaO and the sum of the oxides. In addition, other potentially important anions such as chloride, sulfate, sulfide, and hydroxyl are not detected by this technique and may lead to deficiencies in the analyses. Organic matter is likewise a diluent not measured and can lead to deficiencies in the sum of the oxide concentrations. Iron is reported as Fe_2O_3, which may be incorrect for several reasons. No attempt was made to construct calibration curves by adding either $CaCO_3$ or SiO_2 to the sediment standards. This may lead to erroneous calibrations in the analyses of samples rich in biogenic carbonate and silica, but errors are likely to be small. Sediments are generally a mixture of materials from several sources, and the absolute accuracy required by hard-rock analysts for the calculation

of original liquid compositions and lines of descent are not so important for these analyses. Sample pre-treatment was restricted to drying and grinding. Samples were not ignited and no attempt was made to wash away sea salt. Despite these difficulties, this technique permits routine shipboard analysis of many samples at a level of accuracy and precision sufficient for shipboard sedimentological studies.

PALEOMAGNETISM

Paleomagnetic studies performed on board the *JOIDES Resolution* during Leg 124 included measurements of remanent magnetization (RM) and magnetic susceptibility of the sediments and the basement rocks. Measurement of RM was accompanied by AF (alternating field) demagnetization so that secondary magnetization could be removed. In general, magnetic measurements have produced very good results due to high content of volcanic material in the sediments and the high sedimentation rates in the Celebes and Sulu Seas marginal basins.

Instruments

The instruments in the shipboard paleomagnetic laboratory performed with only minor problems that were resolved during the cruise. Two magnetometers, a Molspin spinner magnetometer and a 2-G Enterprises (model 760R) pass-through cryogenic superconducting rock magnetometer (SRM), were available for measurement of RM. An AF demagnetizer (Model 2G600) capable of AF fields up to 25 mT was in line with the cryogenic SRM. At the beginning of Leg 124 a FASTCOM4 multi-serial communication board was installed in the PC-AT compatible computer so that the PC could be in full automatic control of the SRM, the demagnetizer, and the step motor that transports the core sections. A BASIC program (named SUPERMAG) modified from University of Rhode Island's long-core cryogenic system was used for the measurement of archive-half sections. A modified version of the program (named SUPRCUBE) was developed for measurement of discrete samples.

The SQUID (superconducting quantum interference devices) electronics of the SRM were operating at the 1X scale and using flux-counting mode for most of the measurements (100X for basalt samples). However, for the early measurements made at Site 767, 100X or extended scale without flux counting was used. This was because the y-axis sometimes failed to communicate with the computer and it seemed to fail less frequently in this mode. The communication problem was fixed by replacing the EPROM and other chips within the electronic boxes.

The Molspin spinner, controlled by a DIGITAL PRO 350 computer, measured only discrete samples. The measurement results were found to be consistent with those of the SRM. An error for sample volume correction in the BASIC program for the spinner was found and corrected. We feel that the spinner magnetization intensity data from Leg 109 to Leg 123, therefore, may be as much as two times higher than the correct values.

Remanent Magnetization Measurements

Sediments

RM measurements of the sediments were performed by passing all archive-half sections of the APC cores through the SRM. Measurements were taken at 10-cm intervals at both NRM and one-step demagnetization levels. The selected demagnetization level for a core was determined by progressive demagnetization of one full-length section at 0, 5, 10, and 20 mT. For Site 768 cores, about 200 m of RCB sediment cores were also pass-through measured because individual pieces were longer than the sensor region (20 cm) of the SRM.

At reversal boundaries, high-density measurements at 0.5-cm intervals, at 10, 15, and 20 mT AF demagnetization levels were carried out. Because of the broad SRM sensor region, the measurements contain the averaging effect of the responses of the instrument and, therefore, require deconvolution to recover the higher frequency changes of magnetization. This work will be done later during shore-based studies.

Discrete samples were taken from APC, XCB, and RCB sediment cores. The sampling was done by pressing a plastic box (6 cm^3) into the sediments and removing it with the uphole direction marked on the box. For more consolidated sediments, a saw with two parallel blades was used to cut the cubes. Two to three samples per section were taken in APC, XCB, and RCB cores. The sampling positions in XCB and RCB cores were unevenly distributed, controlled mainly by the distribution of undisturbed portions of the core sections. More than one third of the discrete samples were measured on board with step AF demagnetization at 2, 5, 10, 15, and 20 mT. The SRM was used for most of these measurements. A progressive change in declination (as much as 90°) in individual APC cores occurs very often. In most cases, the declinations at bottom of cores are consistent with the dipole-predicted direction. We believe this is due to rotation of APC core barrels penetrating the sediments.

Basement Rock (basalt)

For the basalt basement cores, minicores of 1-in. (2.54 cm) diameter were taken (averaging one sample per core) and measured with the SRM. The SRM was capable of measuring the stronger basalt samples without problem. Some samples were measured with the spinner and results were consistent with the SRM output. For cores that contain pieces longer than 20 cm, the pieces were measured at 3-cm intervals and step demagnetized to 20 mT. Although the "edge effect" was obvious, the middle part of each of the pieces gave reliable data.

Magnetic Susceptibility Measurement

Magnetic susceptibility measurements were made on all sediment and most basement cores with a Bartington Instrument magnetic susceptibility meter (model M.S.1) with a M.S.1/CX 80-mm whole-core sensor loop set at 0.47 kHz. Due to the high susceptibility of most sediments encountered on the leg, all measurements were made in the low-sensitivity mode.

Measurements were made before splitting, at 10-cm intervals. The data were collected with a DIGITAL PRO 350 microcomputer, uploaded to the shipboard VAX 11/750 computer, processed, and then plotted. During processing, the susceptibility data were examined for top-of-core rust contamination, with suspect data removed before further processing.

In addition to characterizing the cored sediments, susceptibility data were used to correlate between holes and sites. Correlation of susceptibility data was performed by observing peak-to-peak spacings and general trends in the susceptibility curve. Absolute individual peak heights were not useful for correlation of susceptibility data.

BIOSTRATIGRAPHY

General Remarks

The general correlation of the biostratigraphic zones with the magnetic polarity reversal record, the seafloor anomalies, and an absolute time scale is based on the scheme given by Berggren et al. (1985), as modified in ODP Leg 112 (Shipboard Scientific Party, 1988) with a few changes (Fig. 8). Each microfossil zonation was then fit into this reversal/anomaly scheme for the Quaternary to middle Eocene. The minor changes are discussed in the individual chapter for each fossil group.

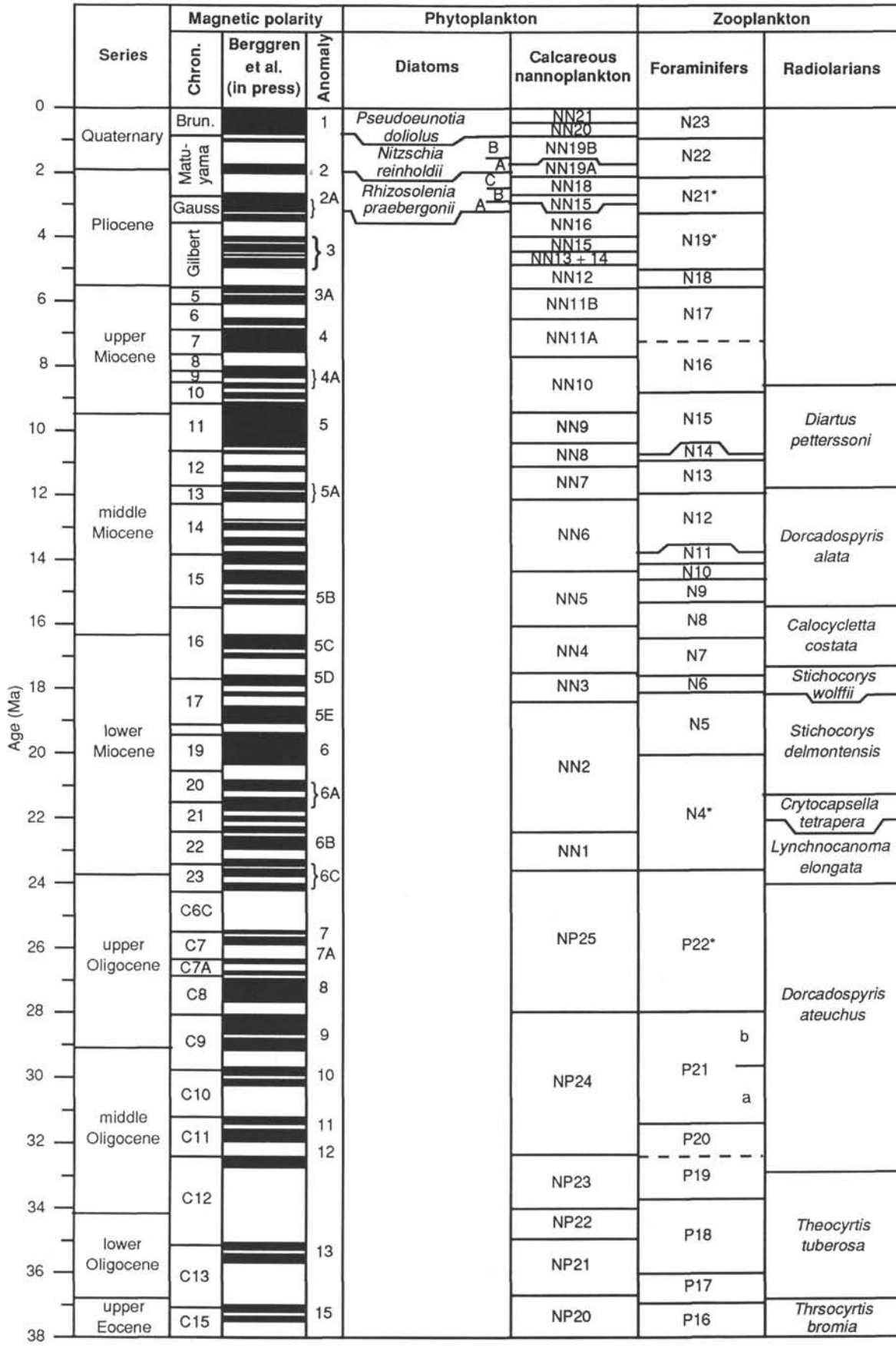

Figure 8. Leg 124 biostratigraphic standard.

Age assignments are mainly based on core-catcher samples. Additional samples were studied to narrow certain time intervals. The location of the samples, the preservation and abundance for each fossil group are indicated in the barrel sheets.

Calcareous Nannofossils

The standard calcareous nannoplankton zonation (Martini, 1971; Martini and Müller, 1986) was used at all sites to identify the nannoplankton zones.

The Miocene/Pliocene boundary is considered to be located at the base of Zone NN12 (Martini and Müller, 1986), and the middle/upper Miocene boundary at the top of Zone NN9.

Nannofossils Abundance and Preservation

Smear slides were prepared from raw sediment for examination of calcarerous nannofossils. The abundance of nannofossils was estimated as follows:

A = abundant (10 specimens/field).
C = common (1–10 specimens/field).
F = few (1 specimen/2–10 fields of view).
R = rare (1 specimen/>100 fields of view).

State of Preservation

G = good, no or only minor signs of dissolution or overgrowth of placoliths and discoasters.
M = moderate, slight to moderate dissolution of placoliths, discoasters, and others or slight to moderate overgrowth, especially on discoasters and other ortholithic forms.
P = poor, severe dissolution in placoliths with abundant broken specimens or heavy overgrowth of discoasters and sphenoliths.

Foraminifers

Planktonic foraminifers, encountered during Leg 124, were zoned using the N- and P-zonation (Blow, 1969). Species-ranges were compiled from Stainforth et al. (1975), Kennett and Srinivasan (1983), and Bolli and Saunders (1987), for the Neogene. Ages for changes in coiling direction in *Pulleniatina* spp. and in *Negaloboquadrina acostaensis* are given by Van Gorsel and Troelstra (1981). Paleogene ranges follow Toumarkine and Luterbacher (1987). The change in coiling direction of *Globorotalia menardii* to dominantly left coiling is slightly younger than the first appearance of *Globorotalia truncatulinoides* (Stainforth et al., 1975), but is here used as a marker for the lower boundary of N22, because *G. truncatulinoides* is too rare to be used. The Pliocene/Pleistocene boundary (1.6 Ma) can approximately be marked by the last occurrence of *Globigerinoides obliquus*. As foraminifers are rare in all Pliocene and older sediments recovered during Leg 124, zonal boundaries cannot be well defined.

All samples were disintegrated in a hot, 10% H_2O_2 solution, with Calgon added to clayey samples, and washed over a 63-μm sieve. The following categories describe the frequencies of planktonic foraminifers in each sample relative to other sand-sized particles:

B = Barren: no foraminifers, or rare arenaceous benthic foraminifers only.
R = Rare: <1% of the residue.
C = Common: 1–25% of the residue.
A = Abundant: >25% of the residue.

The preservation of the foraminifers is described as follows:

G = Good: little or no fragmentation and/or recrystallization.
M = Moderate: some signs of dissolution (fragmentation and dissolution holes) and/or some recrystallization.
P = Poor: severe dissolution and/or recrystallization.
S = Small-sized, sorted: faunas from turbidites that contain small-sized planktonic foraminifers only and/or lack age-diagnostic forms.

Diatoms

With very rare exceptions, Leg 124 sediments contain diatoms only in Quaternary sediments of the *Nitzschia reinholdii* and *Pseudoeunotia doliolus* Zones, according to the low-latitude zonation of Burckle (1972, 1977) and Burckle and Trainer (1979), as summarized and modified by Barron (1985a, b). Good preservation of a diverse diatom assemblage is limited to Holocene muds.

Processing sediments from Leg 124 sites for diatoms proved to be unusually difficult. Diatom abundance is low in nearly all diatom-bearing sediments older than Holocene. All Pleistocene sediments from Leg 124 contain a strong dominance of clay-sized particles. In addition, many samples contain abundant ash, further diluting the diatom assemblage. Separating diatoms from the abundant and frequently strongly flocculated clays without biasing the assemblage required more steps than was practical for shipboard analysis. In most cases standard methods, such as those described by Barron (1985a), proved to be insufficient. For this reason, much of the shipboard diatom study was limited to smear-slide analysis.

Smear slides were prepared with Hyrax on 22 mm × 40 mm cover slips. As many as four smear slides were scanned using at least 400× magnification to evaluate the diatom assemblage. Identifications were made at magnifications of 1000× to 1250×. Diatom abundance was determined from smear slides at 400× magnification according to the following comparison:

A = Abundant: >50 diatoms / transect.
C = Common: 10–50 diatoms / transect.
F = Few: 1–10 diatoms / transect.
R = Rare: 1–32 diatoms / slide.
T = Trace: Only rare fragments of diatoms.
B = Barren: No fragments identifiable as diatom remains seen.

At 400× magnification, each transect consists of about 72 fields of view and the slide contains about 32 transects.

Diatoms were found on a few very rare occasions in >44-μm fractions of sieved residues of radiolarian preparations of Miocene and Oligocene sediments, but diatom abundance is too low in these sediments to recover a useable assemblage from unsieved material.

Radiolarians

Detailed shipboard analysis of radiolarians on Leg 124 was limited to pre-Quaternary successions. Radiolarian assemblages were assigned to biozones initially proposed by Riedel and Sanfilippo (1970, 1971, 1978), and later reviewed by Sanfilippo et al. (1985). Other useful references included Nigrini and Lombardi (1984) and numerous radiolarian studies reported in DSDP *Initial Reports* volumes (most references can be found in Sanfilippo et al., 1985).

Radiolarians are preserved sporadically in Leg 124 sediments—no complete evolutionary sequence was recovered. Most samples containing radiolarians are pelagic or hemipelagic clays with varying proportions of volcanic ash. In general, standard processing techniques were used. A 10-cm^3 sample was soaked in sodium pyrophosphate solution and hydrogen peroxide to disaggregate clays prior to sieving. Often the residue had to be dried and procedures repeated before the sample disaggregated sufficiently.

Several samples were disaggregated using a kerosene/water interaction method. This involves three steps: (1) dry the sample completely, (2) soak the dry sample in kerosene until saturated and (3) replace the kerosene with water by adding a little at a

time. This process was necessary with a few samples that would not respond to the treatment described above, and with samples that contained casts of radiolarians that had been replaced by clay minerals and thus would be damaged by the former process. Acid treatment was necessary only in one thin Paleogene unit cored at Site 770, because carbonate is rare in all other pre-Quaternary sediments of Leg 124.

Samples were sieved using a 44-μm sieve. Residues were embedded in Piccolyte using standard techniques. When the >44-μm fraction contained a large volume of unidentifiable radiolarian fragments, the residue was sieved using a 63-μm screen and mounted as above.

Abundance of radiolarians given in the biostratigraphic sections of the Hole Summaries and Barrel Sheets are based on slides of sieved residues and consequently differ markedly from the lithologic descriptions, which are based on smear-slide data. Abundance estimates are qualitative, determined on the visual approximation of the total amount of residue per 10 cm^3 of sediment and of the percentage of radiolarian specimens observed in this residue. Turbidites and ash-rich layers often left volumes of residues greater than that indicated in the relative abundance scheme described below.

A (abundant) = >1 cm^3 of residue, >80% radiolarians.
C (common) = ~0.1–1 cm^3 of residue, 10%–80% radiolarians.
F (few) = ~0.1–1 cm^3 of residue, 1%–10% radiolarians.
R (rare) = ~0.1–1 cm^3 of residue, <1% radiolarians.
VR (very rare) = ~0.1–1 cm^3 of residue, <1% radiolarians.
— (barren) = no radiolarians in at least one entire slide.

Radiolarian preservation ranges from very poor to excellent. Degraded preservation is a result of recrystallization of opaline silica as quartz and of replacement by clay minerals, zeolites, etc. Preservation is defined as follows:

E = Excellent: Majority of specimens observed are complete with spines intact, no overgrowths or recrystallization.
G = Good: Many specimens complete with spines intact, little or no overgrowths, cement or matrix infill occurs, but outer surface intact. Most specimens determinable.
M = Moderate: A substantial portion of the specimens broken, and some degree of overgrowth, etching or replacement by minerals other than quartz or pyrite. 50% of specimens undeterminable.
P = Poor: Specimens mostly broken and fragmentary or strongly etched or replaced by other minerals. <5% of specimens determinable.
VP = Very poor: Specimens only present as inner molds, casts, or fragments. Positive identification impossible for nearly every specimen.

Ichthyoliths

Age determinations based on ichthyoliths follow Doyle and Riedel (1987). When present, ichthyoliths were picked from the wash-residues scanned for foraminifers; they were then mounted in Canada Balsam. Additional specimens were found in the slides that were prepared for the study of radiolarians. As they are generally rare, larger amounts of sediments were washed than would be done for foraminifers (15–20 cm^3, instead of <5 cm^3). The number of whole specimens was counted in each sample; because the size of the unwashed sample was not determined, this number is converted to semiquantative estimates:

VR = Very rare: less than 10 triangles with tip preserved.
R = Rare: 10–25 triangles.
C = Common: 26 triangles.

The preservation is described as follows:

M = Moderate: faunas consisting of light-brown colored, transparent specimens.
P = Poor: faunas consisting of dark-brown, translucent specimens, many of which are deformed.

The ichthyolith faunas are not rich enough to apply any zonal scheme. Therefore, in the barrel sheets, the presence of selected age-diagnostic types is noted by codes:

I0: No diagnostic forms;
I1: Triangle with triangular projection (Cenozoic);
I2: Small dendritic many radiating lines (upper lower Oligocene–Holocene)
I3: Triangle hooked margin (Eocene–Holocene);
I4: Small triangle crenate margin (Eocene–lower Oligocene);
I5: Narrow triangle cross-hachured (upper Paleocene–lower Miocene);
I6: Flexed triangle shallow inbase ≥ 120 (lower Oligocene–middle Miocene);
I7: Small triangle long striations (Miocene–Holocene);
I8: Flexed triangle 102–112 (upper Oligocene–Holocene).

SEDIMENT INORGANIC GEOCHEMISTRY

Calcium Carbonate

During Leg 124 calcium carbonate determinations were performed on samples taken for physical property determinations. These samples were chosen to represent major lithologic units. To complement this data set, several samples were also taken from carbonate turbidite layers. Sample size was typically 250 mg of freeze-dried sediment. The carbonate content was measured using the CO_2 Coulometer (Coulometrics model 5030). CO_2 was generated by treating the sample with HCl and gentle heating. The evolved CO_2 was transferred to the coulometer by a purified helium stream, where it was quantitatively absorbed, reacting with monoethanolamine to form a titratable acid that caused a color indicator to change. The color change was monitored electronically. As transmittance increased, the titration curve was activated to stoichiometrically generate base at a rate proportional to the transmittance. The titration current was continually measured and integrated to provide CO_2 measurements. Analysis time was 3 to 7 min.

Interstitial Waters

Shipboard interstitial water analyses during Leg 124 were performed on sections of whole-round sediment cores 5 to 10 cm in length. Samples were collected as soon as the core arrived on deck and were taken from every core (about 10 m apart) to a depth of 100 meters below sea floor (mbsf) and from every third core (about 30 m apart) below 100 mbsf. Samples were initially cleaned by scraping off the exterior surface with a stainless steel spatula and then squeezed in a stainless steel press for time periods of up to 2 hr (usually 20 to 30 min) to 40,000 psi at room temperature (Manheim and Sayles, 1974). After filtration through a 0.45-μm filter, the interstitial water samples were analyzed for pH, alkalinity, salinity, chloride, sulfate, calcium, magnesium, silica, ammonium, and phosphate. Alkalinity, pH, and salinity were determined immediately after filtration and samples were then refrigerated and titrations and instrumental analyses performed within a few days after collection.

All shipboard chemical analyses of interstitial waters followed standard ODP techniques. The potentiometric titration of alkalinity and measurement of pH were carried out using a Metrohm autotitrator and a Brinkman combination pH electrode (Gieskes, 1974). The amount of total dissolved salts (salinity) was determined using a Goldberg optical refractometer. Calcium, magnesium, and chloride concentrations were determined titrimetrically as described by Gieskes (1974) and modified by Gieskes and Peretsman (1986). Sulfate was determined using a Dionex ion chromatograph (Gieskes and Peretsman, 1986). Colorimetric methods employing a Bausch and Lomb

Spectronic 1001 spectrophotometer were used to determine the concentration of silica (Gieskes and Peretsman, 1986), ammonium (Solorzano, 1969), and phosphate (Strickland and Parsons, 1968; Presley, 1971). International Association of Physical Sciences Organizations (IAPSO) standard seawater was used to standardize all analyses.

ORGANIC GEOCHEMISTRY

The organic geochemistry program for Leg 124 included: (1) determination of total organic carbon concentrations and characterization of organic matter by Rock-Eval pyrolysis, and (2) analyses of hydrocarbon gases by gas chromatography. Generally, all sediment samples collected for gas analyses were also used for Rock-Eval measurements. In addition several sediment samples were taken for Rock-Eval only. Laboratory and analytical procedures are outlined below. The detailed procedures are described by Emeis and Kvenvolden (1986).

Rock-Eval

The bulk geochemical character of sedimentary organic matter was determined utilizing Rock-Eval-II pyrolysis techniques outlined by Espitalié et al. (1985a, 1985b, 1986). The following parameters were measured during the programmed pyrolysis (300° to 600°C) of 100 mg freeze-dried and ground bulk samples: the amount of "free" hydrocarbons released at 300°C (S1), the amount of hydrocarbons released during heating to 600°C (S2) which is mainly due to cracking of kerogen, total CO_2 released from organic matter during pyrolysis to 390°C (S3), the temperature of maximum hydrocarbon release during pyrolysis (T_{max}); and the total amount of CO_2 generated during oxidation at 600°C. From these values hydrogen, oxygen, productivity indexes, and total organic carbon concentrations were calculated. The hydrogen index represents the ratio of pyrolyzable organic matter or "hydrocarbons" (S2) to total organic carbon (mg HC/g TOC). The oxygen index represents the ratio of carbon dioxide released (S3) to total organic carbon (mg CO_2/g TOC). The production index (PI) is defined as the ratio S1/(S1 + S2). Measurements were carried out on sediments from headspace gas analyses and Rock-Eval samples collected during shipboard sampling.

Hydrocarbon Gases

For safety considerations gas concentrations were monitored in cores at 9-m intervals. Gases were extracted from bulk sediments utilizing headspace or vacutainer sampling techniques (Emeis and Kvenvolden, 1986). Vacutainer gas samples were taken immediately after core retrieval by piercing the core liner and withdrawing gas into a vacuum tube. Voids within the core are sought as sites for gas sampling by this technique. The headspace analyses were performed on about 5 g of sediment that was placed in a glass container sealed with a septum and metal crimp and then heated to 70°C for about 45 min. A 5-cm^3 sample of headspace gas was subsequently injected with a syringe into a gas chromatograph.

All headspace and Vacutainer gas samples were analyzed with a Carle AGC 1000/Model 211. This instrument was designed to measure accurately and rapidly the concentrations of methane, ethane, and propane using a flame ionization Model 3393A integrator that allowed the direct measurement of gas concentrations after appropriate calibration. Occasionally, gases from aliquots of sediments or Vacutainer samples were also measured with a Hewlett-Packard 5890 Natural Gas Analyzer (NGA) if the previous analysis revealed a significant propane concentration. This chromatograph is fitted with Porapak Q, Molecular Sieve and Silicone oil-coated columns, and both thermal conductivity (TCD) and flame ionization (FID) detectors. Gases measured with the NGA during Leg 124 include the suite of C_1–C_6 hydrocarbons. Generally, all gas concentrations are reported in ppm released from 5 g of wet sediment. The details of the configuration of the NGA gas chromatograph are available in Emeis and Kvenvolden (1986).

PHYSICAL PROPERTIES

The shipboard physical properties program provides measurements of the different physical or geotechnical properties of the materials sampled. The physical properties routinely measured on board ship were bulk density, grain density, water content, porosity, compressional-wave velocity, thermal conductivity, and undrained shear strength. Physical properties can assist in the characterization of different lithologic units, provide a verification of downhole geophysical logging results, and provide important constraints on the interpretation of seismic reflection and other geophysical data. Furthermore, physical properties data may be used to estimate the permeability and degree of consolidation, to correct sedimentation rates, and in heat flow calculations. Depth profiles of geotechnical properties may be used for distinguishing lithologic boundaries at drill sites as well as correlating and establishing facies changes between sites.

A discussion of physical property determination with respect to equipment, methods, errors, correction factors, and problems related to coring disturbance was presented by Boyce (1976). The physical properties were influenced by drilling and sampling disturbance and the testing procedures used in the laboratory. For example, the water content of a particular sample could be increased by the drilling fluid (seawater) that often surrounded a disturbed core for many hours prior to a sample being removed from the core for testing.

Samples for physical properties determination were selected from areas of least sample disturbance, and sufficient samples were tested to allow for characterization of all major lithologic units. Typically three discrete samples were selected from each core for index property evaluation, and compressional velocities were often taken on the same samples or in the immediate vicinity of the samples. Samples were choosen to be as representative as possible of the sediment section as a whole; however, occasional samples were taken from thinner layers of markedly different lithologies such as the higher density, carbonate-rich layers often associated with some turbidite deposits. Sample selection and relative frequency depended on the thickness and homogeneity of a particular sequence.

The testing methods employed during Leg 124 are discussed below in the same order in which they were performed on each core. GRAPE, P-Wave logging, and soft-sediment thermal conductivity determination were performed on whole sections of core while the other physical properties measurements were conducted on discrete intervals of the split core.

Gamma-Ray Attenuation Porosity Evaluator (GRAPE)

The Gamma-Ray Attenuation Porosity Evaluator or GRAPE technique is described by Boyce (1976). GRAPE was used to make a continuous measurement of wet-bulk density on whole advanced piston core (APC) and extended core barrel (XCB) cores. Generally, piston cores and only the first few XCB cores were tested as the GRAPE is calibrated for full diameter core. An aluminium standard was used for calibration of the apparatus and was run every second core. The core section to be measured was mounted vertically in a rack, and the gamma-ray source and sensor moved down the length of the core. The attenuation of the gamma rays passing through the liner and core was measured every 1.5 to 2.0 cm, and the bulk density was calculated from the attenuation values. The GRAPE data were filtered to remove those that were the result of gas or gaps and end-cap effects before the data were averaged over 0.2- or 0.5-m intervals. All bulk density data are reported in units of g/cm^3.

Compressional-Wave Velocity Logger (*P*-Wave Logger, or PWL)

The *P*-wave logger operated simultaneously with the GRAPE as both are mounted on the same frame. A short 500-kHz compressional-wave pulse was produced by a transducer at a repetition rate of 1 kHz. A receiving transducer was positioned such that the two transducers were aligned perpendicular to the core axis. A pair of displacement transducers monitor the separation between the compressional-wave transducers, which allows for variations in the outside liner diameter without degrading the accuracy of the velocities. Measurements were taken at 1.5- to 2.0-cm intervals as the transducer moved down the core.

Water was applied to the core liner to improve acoustic contact between the transducers and the liner. As with the GRAPE, only APC and the first few XCB cores were measured, as good quality data can only be obtained on core that completely fills the liner. The deeper XCB cores and all RCB cores had annular voids present between the core and the inside of the liner, which prevented transmission of the compressional waves between the transducers. The PWL data were filtered to remove those that were the result of gas, gaps, and end-cap effects. Additional filtering was performed to eliminate low signal strength data. The lower signal strengths used for filtering were either 100 or 200. The data were finally averaged over 0.2- or 0.5-m intervals prior to plotting the figures. All velocity data are reported in units of km/s.

Technical difficulties were encountered with the PWL equipment at Site 768, and poor PWL data were obtained. Good data were obtained at Site 769 following the repair and calibration of the *P*-wave logger.

Thermal Conductivity

The cores were allowed to equilibrate to room temperature for 2 to 4 hr following GRAPE and PWL, prior to thermal conductivity measurement. The thermal conductivity techniques used are described by Von Herzen and Maxwell (1959) and Vacquier (1985). All thermal conductivity data are reported in units of W/(m·K).

Soft-Sediment Thermal Conductivity

Needle probes connected to a Thermcon-85 unit were inserted into the sediment through holes drilled into the core liner, and the thermal drift was monitored. An additional probe was inserted into a reference material to monitor the probe behavior. Once the temperature had stabilized the probes were heated, and the coefficient of thermal conductivity was calculated as a function of the change in resistance in the probe about every 20 s over a 9- to 12-min interval. When the sediment became too stiff to allow easy insertion of the probe, holes were drilled into the core material prior to insertion of the probes. An attempt was made to insert the probes at locations along each core section that appeared to be the least disturbed. However, an annulus of disturbed sediment and drill fluid was often present along the inside of the liner, which prevented visual identification of the more intact segments in the core.

Hard-Rock Thermal Conductivity

Thermal conductivity measurements on well-lithified sediments and rocks were conducted on split cores with the use of a needle probe partially embedded in a slab of insulating material. The flat surface of a selected sample of split core was polished with 600 grit, then placed on top of the slab. Dow Corning 3 silicone was used to improve the thermal contact between the slab and the sample. The sample and the slab are immersed in a salt-water bath and allowed to reach thermal equilibrium with the water. The probe was heated, and measurements of resistance changes in the probe were made every 9 s for a 9-min interval. The thermal conductivity was determined from the most linear portion of a temperature vs. log-time plot.

Undrained Shear Strength

Undrained shear strength of the sediment described by Boyce (1977) and Lee (1984) was determined using a Wykeham Farrance motorized vane apparatus with a four-bladed vane having a diameter of 1.28 cm and a length of 1.28 cm. The vane was inserted into the split core section perpendicular to its face (i.e., perpendicular to the core axis), to a point where the top of the blade was covered by about 4 to 6 mm of sediment. The vane was then rotated at a rate of about 90° per min until the sediment failed. The undrained shear strength was calculated from the peak torque obtained at failure. Vane rotation was continued for a minimum of 120° to allow for determination of a remolded shear strength. The peak and remolded "torques" were measured from calibrated plots of torque vs. rotation that were generated on a Hewlett-Packard 7015B X-Y Recorder. The vane testing was suspended when radial cracking or other noncylindrical failure surfaces developed around the vane. The noncylindrical failures were observed in the stiffer sediments that had undrained shear strengths exceeding approximately 50 kPa. All shear strengths are reported in units of kPa.

Compressional-Wave Velocity

Compressional-wave velocity measurements, in addition to those described above, were taken on samples that were sufficiently stiff to allow for sampling and provide adequate signal strength. Velocities were calculated from the determination of the traveltime of a 500-kHz compressional wave through a measured thickness of sample, using a Hamilton Frame Velocimeter and Tektronix DC 5010 counter/timer system. Travel distance was measured by using an attached variable resistor (LVT) connected to a Tektronix DM 5010 digital multimeter. Samples were taken by either cutting parallel-sided pieces with a knife in the softer sediments, or using a double-bladed diamond saw for the more brittle or lithified sediments. Basement rock samples were obtained using a double-bladed diamond saw or a 2.5-cm rock corer.

The Hamilton Frame velocity transducers were calibrated with lucite and aluminum standards. The variable resistor was calibrated with standard lengths of aluminum cylinder. Zero traveltimes were measured with the two transducers in contact with the signal amplitude adjusted to 2 V on the oscilloscope. Zero times were taken almost once per core tested. Seawater was used to improve the acoustic contact between the sample and the transducers. Readings of traveltime through samples were taken after the signal amplitude on the oscilloscope had been adjusted to 2 V. When insufficient signal strength was present, velocities from the sample were not recorded. All velocity data are reported in units of km/s.

Index Properties

The index properties of wet-bulk density, grain density, porosity, water content, and void ratio were determined on selected samples of sediment and rock. Many index property samples were previously measured for compressional-wave velocity and this enabled direct correlation between velocity and index properties to check for trends and data consistency. Samples were weighed wet using two calibrated Scientech 202 electronic balances, interfaced with a PRO 350 computer, which compensated for the ship's motion by taking the average of 100 or 111 sample weighings. The wet-sample volumes were then determined by using a Quantachrome helium Penta-Pycnometer. Dry sample weight and volume was determined using the same procedure after freeze drying the sample for at least 12 hr.

The definitions and units used for the index properties are:

1. Porosity (%) = 100 volume of water / volume of wet sediment.
2. Bulk density (g/cm^3) = weight of wet sediment / volume of wet sediment.
3. Grain density (g/cm^3) = weight of dry sediment / volume of dry sediment.
4. Water content (%) = 100 weight of water / dry weight of sediment.
5. Void ratio (unitless) = volume of water / volume of dry sediment. Dry-sediment weights and volumes used in the above calculations were corrected for salt content (assuming seawater salinity of 35‰) by subtracting the estimated weight and volume of residual salt.

Post-Testing Data Presentation

GRAPE, PWL and thermal conductivity data were retrieved from the PRO 350 computers and depths below seafloor were added. In addition the GRAPE and PWL data were filtered and blocked to remove spurious data and to reduce the number of data points. The other physical property data were entered into the shipboard Physical Properties Data Collection System. The system computes the depth below seafloor, index properties, shear strength, and velocities for each sample.

The physical properties collected for samples during Leg 124 are presented in tables and figures in each site chapter. All index property, shear strength, thermal conductivity, and discrete Hamilton Frame velocity data are presented in the tables as well as in the figures. However, the GRAPE and PWL data are only presented in figure form as the number of data points would generate excessively long tables. All tables and figures were generated on a Macintosh computer after uploading the data from the VAX. Porosity (Φ), bulk density (γ), grain density (ρ), water content (wc), and compressional-wave velocity (V_p) values are given in the physical properties column on the barrel sheets for the cores of each site.

PETROLOGY

Core Curation and Shipboard Sampling

Basement rocks recovered during drilling were examined by petrologists to determine whether it was necessary to preserve unique features and/or to expose important structures of the cored material. Otherwise the rocks are split into archive and working halves using a rock saw with a diamond blade. Care is always taken to ensure that orientation is preserved during splitting and prior to labeling, usually by marking the base of each piece with red crayon. Each piece is numbered sequentially from the top of each section, beginning with number 1. Pieces are labeled at the top, on the rounded, not sawn surface. Pieces that can be fitted together (reassembled like a jigsaw puzzle) are assigned the same number, but are lettered consecutively (e.g., 1A, 1B, 1C, etc.). Spacers are placed between pieces with different numbers, but not between those with different letters and the same number. The presence of a spacer may represent a substantial interval of no recovery. Whenever the original unsplit piece is sufficiently large, such that the top and bottom can be distinguished before removal from the core liner (i.e., the piece could not have rotated top to bottom about a horizontal axis in the liner during drilling), an arrow is added to the label pointing to the top of the section. Because pieces are free to turn about a vertical axis during drilling, azimuthal orientation is not possible.

After the core is split, the working half is sampled for shipboard physical properties, magnetics, XRF, XRD, and thin-section studies. These samples may take the form of minicores and, if appropriate, are stored in seawater prior to measurement. Normally samples are taken from each lithologic unit, when recovery permits. The archive half is described in the visual core description (VCD), used for non-destructive physical properties measurements such as magnetic susceptibility, and then photographed before storage.

Visual Core Descriptions

Igneous VCD forms are used in the description of the basement cores (Fig. 9). The left column is a graphic representation of the archive half. A horizontal line across the entire width of the column denotes a plastic spacer glued between rock pieces inside the liner. Oriented pieces are indicated on the form by an upward-pointing arrow to the right of the piece. Shipboard samples and studies are indicated on the VCD in the column headed "shipboard studies," using the following notation: XRD = X-ray diffraction analysis, XRF = X-ray fluorescence analysis, TSB = petrographic thin section.

As igneous rocks are classified mainly on the basis of mineralogy and texture, a checklist of macroscopic features is followed to ensure consistent and complete descriptions. These are later stored on a computerized database that is widely accessible.

To describe fine-grained and medium-grained extrusive rocks and dikes, the core is subdivided into lithologic units using the criteria of changing grain size, occurrence of glassy margins, and changes in petrographic type and phenocryst abundances. For each lithologic unit the following information is recorded:

A.1. Leg, site, hole, core number, core type, and section.

A.2. Unit number (consecutive downhole), rock name, the section(s) and piece numbers making up the complete unit.

A.3. Contact type (e.g., intrusive; discordant; depositional, etc.) and dip, and the presence of any associated glass or its alteration products.

A.4. The number of phenocryst phases and their distribution within the unit. For each phenocryst phase: (i) abundance (%); (ii) average size in mm; (iii) shape; (iv) the degree of alteration; and (v) further comments.

A.5. Groundmass texture: Glassy, microcrystalline, fine-grained (<1 mm), medium-grained (1–5 mm), or coarse-grained (>5 mm). Relative grain size changes within the unit (e.g., coarsening from Piece 1 to Piece 5).

A.6. Color and variation within unit. Colors are coded using the Munsell color chart and recorded when the core is dry.

A.7. Vesicles: Percentage abundance, distribution, size, shape, fillings and their relationships (include proportion of vesicles that are filled by alteration minerals).

A.8. Structure: massive flow, pillow lava, thin flow, breccia, hyaloclastite, etc., and comments.

A.9. Alteration: fresh (<2% altn.), slightly (2%–10% altn), moderately (10%–40% altn), highly (40%–80% altn), very highly (80%–95% altn) or completely (95%–100% altn) altered. Type, form, and distribution of alteration.

A.10. Veins/Fractures: percent present, width, orientation, fillings, and relationships. The relationship of the veins and fractures to the alteration is also noted.

A.11. Comments: notes on the continuity of the unit within the core and the interrelationship of units are added here, when appropriate.

Basalts are termed aphyric, sparsely phyric, moderately phyric, or highly phyric, depending upon the proportion of phenocrysts visible with the hand lens or binocular microscope (approximately 10×). Basalts are called aphyric if phenocrysts clearly amount to less than 1% of the rock, sparsely phyric if phenocryst content ranges from 1%–2%, moderately phyric at 2%–10%, and highly phyric if phenocrysts amount to more than 10% of the rock. Basalts are further classified by phenocryst

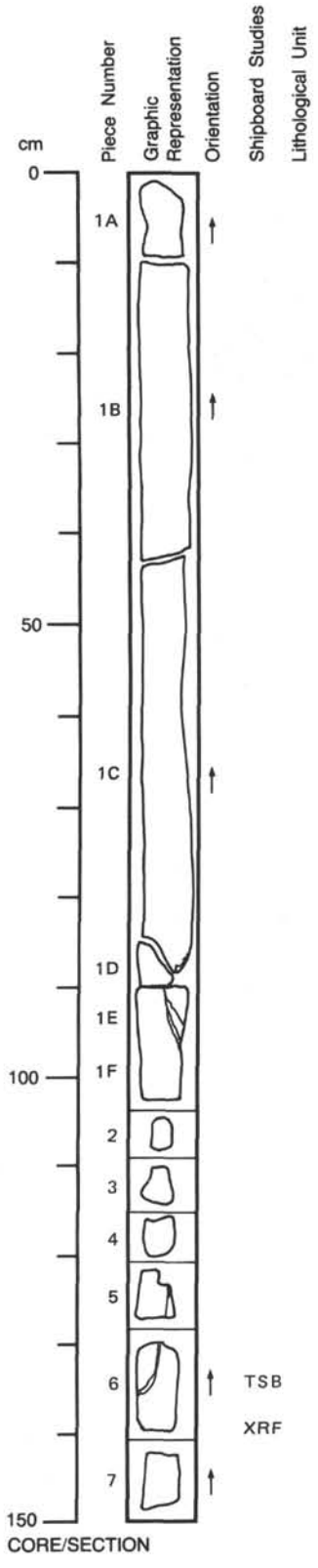

124-768C-91R-1

UNIT 2: CONTINUED

Pieces 1-7

CONTACTS: None.
PHENOCRYSTS: None.
GROUNDMASS: Medium-grained, phaneritic, hypidiomorphic granular rock consisting of 37% skeletal and lath plagioclase 0.07-1.5 mm (An50-70, An70-90), 30% subhedral clinopyroxene 0.04-1.2 mm, 2% olivine, 3% euhedral Fe-Ti oxide 0.008-0.3 mm, and 8% mesostasis.
VESICLES: 20%; 0.4-9.0 mm; Round; Evenly distributed; Filled with clay.
COLOR: Greenish-gray.
STRUCTURE: Massive.
ALTERATION: Moderately altered, clays, allophane, and actinolite replace mesostasis, Fe oxide after olivine and magnetite.
VEINS/FRACTURES: Few.

Figure 9. Sample igneous rocks visual core description form.

type (e.g., a moderately plagioclase-olivine phyric basalt contains 2%–10% phenocrysts, most plagioclase, with subordinate olivine).

Synoptic versions of the Leg 124 igneous VCD forms are published with this volume and are available on microfilm at all three ODP repositories.

Thin-Section Descriptions

Thin-section billets of basement rocks recovered are examined to (a) confirm the identity of petrographic groups in the cores; (b) better understand the textures and interrelationships of the mineral phases; (c) help define unit boundaries indicated by hand specimen core descriptions; and (d) define the secondary alteration mineralogy. Percentages of individual phenocryst phases are estimated and are reported on the detailed thin section description sheets (available in microform at the repositories). The terms "sparsely," "moderately," and "highly" phyric are used in the same manner as for hand specimen descriptions. In cases where discrepancies arise in the lithostratigraphic summary over the composition and abundance of phenocryst phases between hand specimen and thin section analyses, thin-section descriptions are used in preference to hand-specimen descriptions.

X-ray Diffraction (XRD) Analyses

A Philips ADP 3520 X-ray diffractometer is used for the X-ray diffraction (XRD) analysis of mineral phases. Instrument conditions in normal use are as follows:

CuK-alpha radiation with a Ni filter, 40 kV, 35 mA, Goniometer scan from 2° to 70° 2-θ, step size = 0.02°, count time = 1 s per step.

Samples are normally ground using the Spex 8000 Mixer Mill or, when the sample is very small, an agate mortar and pestle is used. The material is then pressed into the sample holders, or smeared on glass plates that were placed in the sample holders, for X-ray analysis.

Resulting diffractograms are interpreted with the help of a computerized search and match routine using Joint Committee on Powder Diffraction Standards (JCPDS) powder files and tabulated data for clay minerals in Brindley and Brown (1980).

X-Ray Fluorescence (XRF) Analysis

Prior to analysis, samples are normally crushed in the Spex 8510 Shatterbox using a tungsten carbide barrel. This produces some tantalum and massive tungsten contamination of the sample. If post-cruise studies for these elements, or instrumental neutron activation analysis are envisaged using the shipboard XRF powders (as on Leg 124), samples are crushed using an agate-lined barrel.

A fully automated wavelength-dispersive ARL8420 XRF system is used to determine the major oxide and trace-element abundances of whole-rock samples. Analyses of the major oxides are carried out on lithium borate glass disks doped with lanthanum as a "heavy absorber" (Norrish and Hutton, 1969). The disks are prepared from 500 mg of rock powder, ignited for 2 hr at about 1030°C, mixed with 6.000 g of dry flux consisting of 80% lithium tetraborate and 20% La_2O_3. This mixture is then melted at 1150°C in a Pt-Au crucible for about 10 min and poured into a Pt-Au mold using a Claisse Fluxer. The 12:1 ratio of flux to sample and the use of the lanthanum absorber make matrix effects insignificant over the normal range of igneous rock compositions. Hence the following linear relationship between X-ray intensity and concentration holds:

$$C_i = (I_i m_i) - b_i$$

where: C_i = concentration of oxide i (wt.%); I_i = net peak X-ray intensity of oxide i; m_i = slope of calibration curve for oxide i (wt %/cps); and b_i = apparent background concentration for oxide i (wt %).

The slope m_i is calculated from a calibration curve derived from the measurement of well-analyzed reference rocks. The background b_i is either determined on blanks or derived by regression analysis from the calibration curves.

Systematic errors due to short-term or long-term fluctuations in X-ray tube intensity are corrected by normalizing the measured intensities of the samples to that of a standard that is always run together with a set of six samples. To reduce weighing errors, two glass disks may be prepared for each sample. Weighing is performed with particular care as it can be a major source of error. Loss on ignition values, if required, are determined by weighing the sample before and after ignition at 1030°C.

Trace-element determinations use pressed-powder pellets prepared by pressing (with 12,000 psi of pressure) a mixture of 5.0 g of dry rock powder (dried at 110°C for >2 hr) and 30 drops of polyvinylalcohol binder into an aluminum cap. A modified Compton scattering technique based on the intensity of the Rh Compton peak was used for matrix absorption corrections (Reynolds, 1967).

An outline of the computation methods is given below.

1. Input X-ray intensities. Dead-time corrected X-ray intensities are read into the program from an Applied Research Laboratory (A.R.L.) result file.

2. Drift corrections. All peak and background intensities are corrected for machine drift by using a one-point correction of the form:

$$D_i = S_i / M_i$$
$$Id_i = I_i D_i$$

Where

D_i = Drift factor for element i, generally 1.00 ± 0.01

S_i = Peak intensity for element i, measured on synthetic standard 'POOP' at time of calibration.

M_i = Measured peak intensity for element i, measured on 'POOP' at anytime after the calibration.

I_i = Uncorrected peak or background intensity, element i.

Id_i = Drift-corrected peak or background intensity, element i.

3. Subtract backgrounds. Correct peak intensities for nonlinear backgrounds by measuring a peak (PK_i) to average background ratio ($AVBg_i$). This is determined for each element, on synthetic and natural blank standards, at time of calibration:

$$BF_i = PK_i / AVBg_i$$

Thus, when measuring unknowns, the true or modified background (MBg_i) is calculated by multiplying the average measured background for element i, ($AVBg_i$) by the BF_i. This new modified background value is then subtracted from the peak intensity (PK_i) to arrive at the net peak intensity ($NETPK_i$) for element i:

$$MBg_i = AVBg_i \cdot BF_i$$
$$NETPK_i = PK_i - MBg_i$$

4. Remove spectral interferences. During calibration, interferences are measured on synthetic pellets containing pure quartz and the interfering element. A ratio of the interference

intensity to the net peak of the interfering element is calculated and assumed constant with respect to concentration. When measuring an unknown, the net interference (INTFERi,j) is calculated and removed by:

$$\text{INTFER}_{i,j} = \text{NETPK}_i \cdot \text{IR}_{i,j}$$
$$\text{CNETPK}_j = \text{NETPK}_j - \text{INTFER}_{i,j}$$

Where

$\text{INTFER}_{i,j}$ = the net interference intensity of element i on element j, and
CNETPK_j = the net intensity of element j with the interference element i removed.

In the case of mutually interfering elements, an iterative approach to this same calculation is used until all the elements involved converge on their respective corrected values.

5. Measure mass absorption coefficients. To correct for matrix differences between samples, three separate mass absorption coefficients are determined following a modification of the Compton scattering technique of Reynolds (1967). Measured intensities from the rhodium K-series Compton, FeKa, and TiKa lines are compared to the calculated absorption coefficients of Rb (ARb), Cr (ARb), and V (AV) respectively. From this comparison, three equations can be written to describe the relationship between each coefficient and its respective line.

6. Calculate concentrations. Once all spectral and matrix corrections have been calculated, the equation to calculate elemental concentrations reduces to:

$$C_i = (\text{CNETPK}_i + A_i) / K_i$$

Where

C_i = *concentration of element i* in parts per million;
CNETPK_i = corrected net peak intensity, element i;
A_i = mass absorption coefficient for element i; and
K_i = Calibration factor (ppm/cps) for element i. K_i is analogous to the calibration curve slope (m_i) for major elements and is determined in the same manner on natural rock and mineral standards.

Details of the analytical conditions for each element determined are given in Table 4.

Some XRF analyses made on board have been repeated on an aliquot of the analyzed powder at the University of Udine, Italy. The method used at Udine for major-element determination is modified from ODP technique by using lithium borate glass disks without absorber.

DOWNHOLE MEASUREMENTS

Tool Strings

Downhole logging directly determines physical and chemical properties of formations adjacent to the borehole. Interpretation of these continuous, *in-situ* measurements can yield a stratigraphic, lithologic, geophysical, and mineralogic characterization of the site. After coring is completed at a hole, a tool string is lowered downhole on a 7-conductor cable, and each of several tools in the tool string continuously monitors some property of the adjacent borehole. Of the dozens of different tool strings commonly used in the petroleum industry, three Schlumberger tool strings were used on Leg 124: the seismic stratigraphic, lithoporosity, and geochemical combinations. Three additional tools were run: L-DGO borehole televiewer, L-DGO temperature, and Miami packer.

The seismic stratigraphic combination used on Leg 124 is a digital string, consisting of long-spaced sonic (LSS), natural gamma-ray tool (NGT), and phasor induction (DIT). A mechanical caliper device (MCD) was included on this string at Site 767. This tool combination measures compressional-wave velocity and provides indicators of the two variables that most often control velocity: porosity, as indicated by resistivity, and clay content, as indicated by the natural gamma tool.

The lithoporosity combination consists of the NGT, neutron porosity (CNT-G), and lithodensity (LDT). On Leg 124 this tool string also included the general-purpose inclinometer (GPIT). This combination provides measurements of formation porosity and density, and determines the spectral content of naturally occurring radiation.

The geochemical combination normally consists of the NGT, aluminum clay tool (ACT), and gamma spectrometry tool (GST). This tool combination measures the relative concentrations of 13 elements: silicon, calcium, aluminum, iron, sulfur, manganese, hydrogen, chlorine, titanium, gadolinium, potassium, thorium, and uranium.

Logs

A brief description of logging tools run during Leg 124 is given in the following. A detailed description of logging tool principles and applications is provided in Schlumberger (1972), Serra (1984), and Timur and Toksoz (1985).

Electrical Resistivity

The dual induction tool (DIT-E) provides three different measurements of electrical resistivity, each one with a different depth of investigation. Two induction devices (deep and medium resistivity) send high-frequency alternating currents through transmitter coils, creating magnetic fields that induce secondary (Foucault) currents in the formation. These ground-loop currents produce new inductive signals, proportional to the conductivity of the formation, which are recorded by the receiving coils. Measured conductivities then are converted to resistivity. A third device (spherically focused resistivity) measures the current necessary to maintain a constant voltage drop across a fixed interval. Vertical resolution is around 2 m for the medium- and deep-resistivity devices and about 1 m for the focused resistivity.

Water content and salinity are by far the most important factors controlling the electrical resistivity of rocks. To first order, resistivity responds to the inverse square root of porosity (Archie, 1942). Other factors influencing resistivity include the concentration of hydrous and metallic minerals, vesicularity, and geometry of interconnected pore space.

Sonic Velocity

The long-spaced sonic (LSS) tool uses two acoustic transmitters and two receivers to measure the time required for sound waves to travel over source-receiver distances of 2.4, 3.0, and 3.6 m. The raw data are expressed as time required for a sound wave to travel through 0.31 m of formation; these traveltimes are then converted to sonic velocities. First arrivals for the individual source-receiver paths are used to calculate the velocities of the different waves traveling in the formation (compressional, shear, etc.). Only compressional-wave velocity is determined during data acquisition, but waveforms are recorded for post-cruise determination of shear-wave velocities and possibly improved compressional-wave velocities. The vertical resolution of the tool is 0.61 m. Compressional-wave velocity is dominantly controlled by porosity and lithification; decreases in porosity and increases in lithification cause the velocity to increase.

Table 4. Leg 124 X-ray fluorescence analytical conditions.

Element	Line	Crystal	Detector	Collimator	Peak angle (deg)	Background offset (deg)	Total count time (s)	
							Peak	Background
SiO_2	Kα	PET(002)	FPC	Coarse	109.25	0	40	0
TiO_2	Kα	LIF(200)	FPC	Fine	86.14	0	40	0
Al_2O_3	Kα	PET(002)	FPC	Coarse	145.27	0	100	0
[a]Fe_2O_3	Kα	LiF(200)	FPC	Fine	57.52	0	40	0
MnO	Kα	LiF(200)	KrSC	Fine	62.98	0	40	0
MgO	Kα	TLAP	FPC	Coarse	44.87	±0.80	200	200
CaO	Kα	LiF(200)	FPC	Coarse	113.16	0	40	0
Na_2O	Kα	TLAP	FPC	Coarse	54.71	−1.20	200	200
K_2O	Kα	LiF(200)	FPC	Fine	136.65	0	40	0
P_2O_5	Kα	Ge(111)	FPC	Coarse	140.94	0	100	0
Rh	K-C	LiF(200)	Scint	Fine	18.59	0	100	0
Nb	Kα	LiF(200)	Scint	Fine	21.37	±0.35	200	200
Zr	Kα	LiF(200)	Scint	Fine	22.53	±0.35	100	100
Y	Kα	LiF(200)	Scint	Fine	23.78	±0.40	100	100
Sr	Kα	LiF(200)	Scint	Fine	25.13	±0.40	100	100
Rb	Kα	LiF(200)	Scint	Fine	26.60	±0.60	100	100
Zn	Kα	LiF(200)	Scint	Fine	41.79	±0.40	60	60
Cu	Kα	LiF(200)	Scint	Fine	45.02	±0.40	60	60
Ni	Kα	LiF(200)	Scint	Coarse	48.67	±0.60	60	60
Cr	Kα	LiF(200)	FPC	Fine	69.35	±0.50	60	60
Fe	Kα	LiF(220)	FPC	Fine	85.37	−0.40+0.70	40	40
V	Kα	LiF(220)	FPC	Fine	122.84	−0.50	60	60
TiO_2	Kα	LiF(200)	FPC	Fine	86.14	±0.50	40	40
[b]Ce	Lα	LiF(220)	FPC	Coarse	127.92	±1.50	100	100
[b]Ba	Lα	LiF(220)	FPC	Coarse	128.53	±1.50	100	100

[a] Total Fe as Fe_2O_3.
[b] Calibrated, but not analyzed on basalts.
Note: FPC = Flow proportional counter using P10 gas; KrSC = Sealed Krypton gas counter; Scint = NaI scintillation counter. All elements were analyzed under vacuum on goniometer 1, at generator settings of 60 kV and 50 mA.

Natural Gamma Ray

The natural gamma-ray tool (NGT) measures the natural radioactivity of the formation. Most gamma rays are emitted by the radioactive isotope ^{40}K and by the radioactive elements of the U and Th series. The gamma-ray radiation originating in the formation close to the borehole wall is measured by a scintillation detector mounted inside the sonde. The analysis is achieved by subdividing the entire incident gamma-ray spectrum into five discrete energy windows. The total counts recorded in each window, for a specified depth in the well, are processed at the surface to give the elemental abundances of K, U, and Th.

Because radioactive elements tend to be most abundant in clay minerals, the gamma-ray curve is commonly used to estimate the clay or shale content. There are rock matrixes, however, for which the radioactivity ranges from moderate to extremely high values as a result of the presence of volcanic ash, potassic feldspar, or other radioactive minerals.

Mechanical Caliper Device

The mechanical caliper device (MCD) provides a basic two-dimensional caliper log of the borehole by means of a bow-spring-mounted measurement system. The hole diameter (HD) log is used to detect washouts or constrictions. Borehole diameter significantly affects many of the other logging measurements, and the hole diameter is an important input to log correction routines.

Lithodensity Tool

The lithodensity tool (LDT) uses a ^{137}Ce gamma-ray source to measure the resulting flux at fixed distances from the source. Under normal operating conditions, attenuation of gamma rays is chiefly caused by Compton scattering (Dewen, 1983). Formation density is extrapolated from this energy flux by assuming that the atomic weight of most rock-forming elements is approximately twice the atomic number. A photoelectric effect index is also provided. Photoelectric absorption occurs in the energy window below 150 keV and depends on the energy of the incident gamma ray, the atomic cross section, and the nature of the atom. Because this measurement is almost independent of porosity, it can be used directly as a matrix lithology indicator. The radioactive source and detector array is placed in a tool that is pressed against the borehole wall by a strong spring. Excessive roughness of the hole will cause some drilling fluid to infiltrate between the skid and the formation. As a consequence, density readings can be artificially low. Approximate corrections can be applied by using caliper data. The vertical resolution is about 0.30 m.

Compensated Neutron Porosity

A radioactive source mounted on the compensated neutron porosity tool (CNT) sonde emits fast neutrons (4 MeV) into the formation, where they are scattered and slowed by collisions with other nuclei. When the neutrons reach a low energy level (0.025 MeV), they are captured and absorbed by atomic nuclei such as hydrogen, chlorine, silicon, and boron. The scattering cross-section is the quantity that describes the rate at which neutrons are slowed. Because the scattering cross-section for hydrogen is about 100 times larger than for any other common element in the crust, most energy dissipation is caused by collisions with water molecules. Therefore, a change in the number of neutrons detected at a receiver can be related to porosity. In practice, an array of detectors is used to minimize borehole or drilling fluid effects. Because water is present both in pores and as bound water (e.g. clay minerals), porosity measurements made in the presence of hydrous minerals are overestimates of the true

porosity. The vertical resolution of the tool is theoretically about 0.25 m, but low signal-to-noise ratio degrades this potential resolution.

Gamma Spectrometry Tool

This induced spectral gamma-ray tool (GST) consists of a pulsed source of 14-MeV neutrons and a gamma-ray scintillation detector. A surface computer performs spectral analysis of gamma rays resulting from the interactions of neutrons emitted by the source with atomic nuclei in the formation (Hertzog, 1979). Characteristic sets of gamma rays from six elements dominate the spectrum, permitting shipboard calculation of six elemental yields: Ca, Si, Fe, Cl, H, and S. As their sum is always one, they do not reflect the actual elemental composition. Therefore, ratios of these yields are commonly used in interpreting the lithology, porosity, and salinity of the formation fluid.

Aluminum Clay Tool

Aluminum abundance as measured by the Aluminum Clay Tool (ACT) is determined by neutron-induced (Cf chemical source) late gamma-ray spectrometry. By placing NaI detectors both above and below the neutron source, contributions from natural gamma-ray activity can be removed. Calibration to elemental weight percent is performed by taking irradiated core samples of known volume and density and measuring their gamma-ray output while placed in a jig attached to the logging tool (generally after logging).

Borehole Televiewer

The borehole televiewer (BHTV) is an ultrasonic, high-resolution logging tool utilized to measure the geometry of the borehole wall, fractures, and lithostratigraphic features. The televiewer contains a rotating acoustic transducer that emits a focused 3° beam pulse at a rate of 1800 times a second. The transducer rotates three times per second. Two transducers permit the BHTV to operate in either low-frequency (400 kHz) or high-frequency (1.4 MHz) mode. Both frequencies were used on Leg 124. The high-frequency transducer is designed to resolve detailed features such as fracture density and fracture aperture. The orientations of all features are determined with a fluxgate magnetometer that triggers the signal at each crossing of magnetic north while the tool is pulled uphole at a rate of 2.5 cm/s. A reflectance image of the borehole wall is obtained in real time by windowing the acoustic reflection off the borehole wall and recording this on Polaroid film. The raw output consists of full waveform acoustic seismograms that are also recorded on videotape for later reprocessing. The traveltimes and the degree of acoustic reflectance from these data can then be used to determine a more accurate 3-D image of the borehole geometry, as well as delineate the textural characteristics of the borehole wall.

Temperature Tool

The L-DGO temperature tool is a self-contained tool that can be attached to any Schlumberger tool string or to the televiewer. Data from two thermistors and a pressure transducer are collected every 0.5–5.0 s and stored in a Tattletale computer within the tool. Following the logging run, data are transferred from the Tattletale to the Masscomp computer for analysis. A fast-response thermistor, though low in accuracy, is able to detect sudden very small temperature excursions caused by fluid flow from the formation. A slow-response thermistor has high accuracy and can be used to estimate heat flow. Data are recorded as a function of time; conversion to depth can be based on the pressure transducer or, preferably, on simultaneous recording by Schlumberger of both depth and time.

Log Data Quality

Log data quality may be seriously degraded in excessively large sections of the borehole or by rapid changes in the hole diameter. Resistivity and velocity measurements are less sensitive to borehole effects, whereas the nuclear measurements (density, neutron porosity, and both natural and induced spectral gamma ray) are most seriously impaired because of the large attenuation by the borehole fluid. Corrections can be applied to the original data to reduce the effects of these conditions and, generally, any departure from the conditions under which the tool was calibrated.

Different logs may have small depth mismatches, caused by either cable stretch or ship heave during recording. Small errors in depth matching can impair the results in zones of rapidly varying lithology. To minimize such errors, a hydraulic heave compensator adjusts for rig motion in real time. The heave compensator was not used on Leg 124 because seas were generally calm. Precise depth matching of logs with cores is not obtainable in zones where core recovery is low because of the inherent ambiguity of placing the recovered section within the interval cored.

Log Analysis

During logging, incoming data were observed in real time on a monitor oscilloscope and simultaneously recorded on digital tape in either the Schlumberger logging unit or Downhole Measurements Laboratory. After logging, the Schlumberger tape was read by the Masscomp computer system in the Downhole Measurements Laboratory and reformatted to a file format compatible with the Terralog log-interpretation software package. Rather than being a "black box," Terralog is an interactive system consisting of many log manipulation and plot options. Thus, the log analysis and interpretation varied in duration and procedure for each site. Most log interpretation was carried out aboard ship; further analysis and interpretation were undertaken after the cruise, using a companion system in the Borehole Research Laboratory of Lamont-Doherty Geological Observatory.

Reprocessing of Logs

Raw GST logs for Leg 124 are shown following the barrel sheets for each site at which the GST was run. Raw count rates for six elements (Ca, Si, Fe, S, Cl, and H) are obtained in real time by the Schlumberger data acquisition software. These count rates commonly exhibit some inversion interference of chlorine with other elemental count rates, which is manifest as a strong but spurious correlation between chlorine and calcium, and weaker correlations with other elements measured by the tool. This interference, which is attributable to the dominance of the induced gamma spectrum by chlorine, is unavoidable in ODP holes because the minimum pipe diameter is too small to permit use of a boron sleeve for chlorine count suppression. Most of this interference effect was removed aboard ship by adding to each count-rate log the product of chlorine counts and the slope of a first-degree regression with chlorine.

The shipboard correction was not utilized in post-cruise reprocessing, using a Schlumberger Elite 1000 workstation and proprietary Schlumberger software. With a revised algorithm, the gamma spectrum at each depth is inverted for titanium, gadolinium, and potassium in addition to the six elements (Ca, Si, Fe, S, Cl, and H) in the shipboard inversion. Though gadolinium is present in concentrations of only a few parts per million, its neutron capture cross-section is so large that gadolinium can account for 10–30% of the total gamma spectrum. Inclusion of these additional elements improves the quality of the

overall inversion, particularly improving the accuracy of calculated calcium abundance, by converting sources of unaccounted variance to signals. However, the potassium concentrations determined are less accurate than those from the NGT, and the hydrogen concentrations are less accurate than those from the neutron tool.

Aluminum concentrations from the ACT require only one correction, an adjustment for variations in cable speed. Changes in logging speed affect the time lag between neutron irradiation of the formation and recording of the induced gamma spectrum because the number of induced gamma rays decreases rapidly with time. Post-cruise correction was made based on the cable speed recorded during logging. However, the small amount of ship heave during logging may make this correction less reliable in ODP holes than in land wells.

When all three Schlumberger tool strings are run, further reprocessing of geochemical logs is possible. The relative abundances of Ca, Si, Fe, Ti, Al, K, S, Th, U, and Gd are used to calculate a log of predicted photoelectric effect. The difference between this log and the actual log of photoelectric effect can be attributed to the only two major elements not directly measured, Mg and Na. Major elements are converted from volume percent to weight percent using logs of total porosity (bound water plus pore water) and density. Major elements are expressed in terms of oxide dry weight percent, based on the assumption that oxygen is 50% of the total dry weight. Site 770 was the only Leg 124 site where three-tool strings were run and, thus, for which these procedures are feasible.

If GST data are available but not enough log types are run to permit complete solution for oxide weight percentage, one further processing step is made. Omitting chlorine and hydrogen, the yields of the other GST elements (Ca, Si, Fe, Ti, S, K, and Gd) are summed, and each is expressed as a fraction of this total yield. This procedure corrects for porosity and count rate variations. Although the absolute abundance of each element is not determined, downhole variations in relative abundance are indicated.

Sonic logs obtained in real time are not based on full-waveform analysis, but on a thresholding technique that attempts to detect the compressional wave arrival by a first-break criterion. Occasionally this technique fails and either the threshold is exceeded by noise or the first compressional arrival is below the threshold. This phenomenon, called cycle skipping, creates spurious spikes on the sonic log. On Leg 124, raw traveltimes were reprocessed with an algorithm designed to reject cycle skips (Shipboard Scientific Party, 1987). This algorithm was expanded to include calculation of a caliper log, based on Snell's law and the fact that the observed total source-receiver traveltime is a sum of the known refracted-wave traveltime through the formation and unknown traveltime in the borehole. Though the resulting caliper log is sensitive to assumed fluid velocity, it is probably superior to the hole diameter measured by the caliper tool. The caliper tool used in ODP is subject to sticking when formation mud gets into its mechanical parts, resulting in bimodal (fully open or nearly fully closed) readings.

Synthetic Seismograms

Synthetic seismograms are generated from logging data obtained with the long-spaced sonic (LSS) tool. The bulk density log from the lithodensity tool or a pseudodensity log created from other logs is required in addition to the slowness log. In many cases, a simple constant-density log can be utilized. Experience shows that this often gives surprisingly good results, because both velocity and density are usually controlled by the same parameter: porosity. When velocity and density are highly correlated, synthetic seismograms using a constant density log or an actual density log are virtually identical.

The slowness and density logs are used in the program, which generates an impedance log (velocity – density) that is convolved with a zero-phase Ricker wavelet. The frequency of this wavelet can be varied depending on the source that generated the original seismic profile. A 30-Hz wavelet is capable of a vertical resolution on the order of 30 m, so reflectors cannot generally be attributed to any small-scale lithologic horizons. The synthetic seismogram is plotted with two-way traveltime on the left scale and depth below seafloor on the right. The plot is scaled to uniform time spacing, not uniform depth spacing.

In-Situ Stress Measurements

The borehole televiewer was used on Leg 124 for detecting stress direction from borehole breakouts. Stress-induced wellbore breakouts are elongated zones of spalling along cylindrical holes in rocks. They commonly span a few tens of degrees of circumference. In an isotropic, linearly elastic rock subject to differential stresses, breakouts form along the borehole wall as a result of compressive stress concentrations exceeding the strength of the rock. Under these conditions the breakout orientation will develop in the direction of the least principal horizontal stress. It has been demonstrated in different areas that stress orientations deduced from breakouts are consistent with other independent indicators (Bell and Gough, 1979; Zoback and Zoback, 1980, 1988; Shamir et al., in press; Zoback et al., 1988). Differential horizontal stresses that do not cause failure of the borehole wall can cause borehole ellipticity. Ellipticity is also detectable with the borehole televiewer.

REFERENCES

Archie, G. E., 1942. The electrical resistivity log as an aid in determining some reservoir characteristics. *J. Pet. Tech.*, 5:1–8.

Barron, J. A., 1985a. Late Eocene to Holocene diatom biostratigraphy of the equatorial Pacific Ocean, Deep Sea Drilling Project Leg 85. *In* Mayer, L., Theyer, F., et al., *Init. Repts. DSDP*, 85: Washington (U.S. Govt. Printing Office), 413–456.

_____, 1985b. Miocene to Holocene planktic diatoms. *In* Bolli, H. M., Saunders, J. B., and Perch-Nielsen, K. (Eds.), *Plankton Stratigraphy*: Cambridge (Cambridge Univ. Press), 763–810.

Bates, R. L., and Jackson, J. A., 1980. *Glossary of Geology* (2nd ed.): Falls Church, VA (Am. Geol. Inst.).

Bell, J. S., and Gough, D. I., 1979. Northeast-southwest compressive stress in Alberta: evidence from oil wells. *Earth Planet. Sci. Lett.*, 45:475–482.

Berggren, W. A., Kent, D. V., Flynn, J. J., and Van Couvering, J. A., 1985. Cenozoic geochronology. *Geol. Soc. Am. Bull.*, 96:1407–1418.

Biscaye, P. E., 1965. Mineralogy and sedimentation of recent deep-sea clays in the Atlantic Ocean and adjacent seas and oceans. *Geol. Soc. Am. Bull.*, 76:803–832.

Bizon, G., and Müller, C., 1977. Remarks on some biostratigraphic problems in the Mediterranean Neogene. *In* Biju-Duval, B., and Montadert, L. (Eds.), *Structural History of the Mediterranean Basins*. 25th Congr. CIESM, Split 1976. Paris (Technip), 381–390.

Blow, W. H., 1969. Late middle Eocene to Recent planktonic foraminiferal biostratigraphy. *In* Renz, H. H., and Brönnimann, P. (Eds.), *Proc. Int. Conf. Planktonic Microfossils Geneva, 1967*, 1:199–422.

Bolli, H. M., and Saunders, J. B., 1987. Oligocene to Holocene low latitude planktic foraminifera. *In* Bolli, H. M., Saunders, J. B., and Perch-Nielsen, K. (Eds.), *Plankton Stratigraphy*: Cambridge (Cambridge Univ. Press), 155–262.

Boyce, R. E., 1976. Definition and laboratory techniques of compressional sound velocity parameters and wet-water content, wet-bulk density, and porosity parameters by gravimetric and gamma ray attenuation techniques. *In* Schlanger, S. O., Jackson, E. D., et al., *Init. Repts. DSDP*, 33: Washington (U.S. Govt. Printing Office), 931–958.

Boyce, R. E., 1977. Deep Sea Drilling Project procedures for shear strength measurements of clay sediment using modified Wykeham-Farrance laboratory vane apparatus. *In* Barker, P. E., Dalziel, I.W.D., et al., *Init. Repts. DSDP*, 36: Washington (U.S. Govt. Printing Office), 1059–1068.

Brindley, G. W., and Brown, G. (Eds.), 1980. *Crystal Structures of Clay Minerals and Their X-ray Identification*: London (Mineral. Soc.).

Burckle, L. H., 1972. Late Cenozoic diatom zones from the eastern equatorial Pacific. *Nova Hedwigia*, 39:217–246.

_____, 1977. Pliocene and Pleistocene diatom datum levels for the equatorial Pacific. *Quat. Res.*, 7:330–340.

Burckle, L. H., and Trainer, J., 1979. Middle and late Pliocene diatom datum levels from the central Pacific. *Micropaleontology*, 25:281–293.

Dewen, J. T., 1983. *Essentials of Modern Open Hole Log Interpretations*: Tulsa (Penwall).

Doyle, P. S., and Riedel, W. R., 1987. Cenozoic and Late Cretaceous ichthyoliths. *In* Bolli, H. M., Saunders, J. B., and Perch-Nielsen, K. (Eds.), *Plankton Stratigraphy*: Cambridge (Cambridge Univ. Press), 965–995.

Dunham, R., 1962. Classification of carbonate rocks according to depositional texture. *In* Ham, W. E. (Ed.), *Classification of Carbonate Rocks*: Tulsa (AAPG), 108–121.

Emeis, K.-C., and Kvenvolden, K. A., 1986. Shipboard organic geochemistry on JOIDES Resolution. *ODP Tech. Note*, No. 7.

Espitalie, J., Deroo, G., and Marquis, F., 1985a. La pyrolyse Rock-Eval et ses applications. *Rev. Inst. Fr. Pet.*, 40:563–579.

_____, 1985b. La pyrolyse Rock-Eval et ses applications. *Rev. Inst. Fr. Pet.*, 40:755–784.

_____, 1986. La pyrolyse Rock-Eval et ses applications. *Rev. Inst. Fr. Pet.*, 41:73–89.

Fisher, R. V., and Schmincke, H.-U., 1984. *Pyroclastic Rocks*: New York (Springer-Verlag).

Gieskes, J. M., 1974. Interstitial water studies, Leg 25. *In* Simpson, E.S.W., Schlich, R., et al., *Init. Repts. DSDP*, 25: Washington (U.S. Govt. Printing Office), 361–394.

Gieskes, J. M., and Peretsman, G., 1986. Water-chemistry procedures aboard *JOIDES Resolution*—some comments. *ODP Tech. Note*, No. 5.

Hertzog, R., 1979. Laboratory and field evaluation of an inelastic-neutron-scattering and capture gamma ray spectroscopy tool. *Soc. Pet. Eng. Pap.*, 7430.

Kennett, J. P., and Srinivasan, M. S., 1983. *Neogene Planktonic Foraminifera: A Phylogenetic Atlas*: Stroudsburg, PA (Hutchinson Ross).

Lee, H. J., 1984. State of the art: laboratory determination of strength of marine soils. *In* Chaney, R. C., and Demars, K. R. (Eds.), *Strength Testing of Marine Sediments: Laboratory and In-Situ Measurements*, ASTM Spec. Tech. Publ., 883.

Manheim, F. T., and Sayles, F. L., 1974. Composition and origin of interstitial waters of marine sediments based on deep sea drill cores. *In* Goldberg, E. D. (Ed.), *The Sea* (Vol. 5): New York (Wiley-Interscience), 527–568.

Martini, E., 1971. Standard Tertiary and Quaternary calcareous nannoplankton zonation. *Proc. 2nd Plankton. Conf., Roma 1970*, 2:739–785.

Martini, E., and Müller, C., 1986. Current Tertiary and Quaternary calcareous nannoplankton stratigraphy and correlations. *Newsl. Stratigr.*, 16:99–112.

Mazzullo, J. M., Meyer, A., and Kidd, R., 1987. New sediment classification scheme for the Ocean Drilling Program. *In* Mazzullo, J., and Graham, A. G., *Handbook for Shipboard Sedimentologists*: *ODP Tech. Note*, 8:45–67.

McKee, E. D., and Weir, G. W., 1953. Terminology for stratification and cross-stratification in sedimentary rocks. *Geol. Soc. Am. Bull.*, 64:381–390.

Munsel Soil Color Chart, 1975. Kollmorger Corp., Baltimore, MD.

Nigrini, C., and Lombardi, G., 1984. *A Guide to Miocene Radiolaria: Spec. Publ. Cushman Found. Foraminiferal Res.*, 22.

Norrish, K., and Hutton, J. T., 1969. An accurate X-ray spectrographic method for the analysis of a wide range of geological samples. *Geochim. Cosmochim. Acta*, 33:431–453.

Presley, B. J., 1971. Techniques for analyzing interstitial water samples. Part 1: Determination of selected minor and major inorganic constituents. *In* Winterer, E. L., Riedel, W. R., et al., *Init. Repts. DSDP*, 7, Pt. 2: Washington (U.S. Govt. Printing Office), 1749–1755.

Reynolds, R. C., 1967. Estimation of mass absorption coefficients by Compton scattering: improvements and extensions of the method. *Am. Mineral.*, 52:1493–1502.

Riedel, W. R., and Sanfilippo, A., 1970. Radiolaria, Leg 4, Deep Sea Drilling Project. *In* Bader, R. G., Gerard, R. D., et al., *Init. Repts. DSDP*, 4: Washington (U.S. Govt. Printing Office), 503–575.

_____, 1971. Cenozoic radiolaria from the western tropical Pacific, Leg 7. *In* Winterer, E. L., Riedel, W. R., et al., *Init. Repts. DSDP*, 7, Pt. 2: Washington (U.S. Govt. Printing Office), 1529–1672.

_____, 1978. Stratigraphy and evolution of tropical Cenozoic radiolarians. *Micropaleontology*, 24:61–96.

Sanfilippo, A., Westberg-Smith, M. J., and Riedel, W. R., 1985. Cenozoic radiolaria. *In* Bolli, H. M., Saunders, J. B., and Perch-Nielsen, K. (Eds.), *Plankton Stratigraphy*: Cambridge (Cambridge Univ. Press), 631–712.

Schlumberger, Inc., 1972. *Log Interpretation: Vol. 1, Principles*: New York (Schlumberger).

Serra, O., 1984. *Fundamentals of Well Log Interpretation: Vol. 1. The Acquisition of Logging Data*: Amsterdam (Elsevier).

Shamir, G., Zoback, M. D., and Barton, C. A., in press. *In-situ* stress orientation near the San Andreas Fault: preliminary results to 2.1 km depth from the Cajon Pass scientific drill hole. *Geophys. Res. Lett.*

Shepard, F., 1954. Nomenclature based on sand-silt-clay ratios. *J. Sediment. Petrol.*, 24:151–158.

Shipboard Scientific Party, 1987. Site 645. *In* Srivastava, S., Arthur, M. A., et al., *Proc. ODP, Init. Repts.*, 105: College Station, TX (Ocean Drilling Program), 61–418.

Shipboard Scientific Party, 1988. Explanatory Notes. *In* Suess, E., von Huene, R., et al., *Proc. ODP, Init. Repts.* 112: College Station, TX (Ocean Drilling Program), 25–44.

Solorzano, L., 1969. Determination of ammonia in natural waters by phenol-hypochloridite method. *Limnol. Oceanogr.*, 14:799–801.

Stainforth, R. M., Lamb, J. L, Luterbacher, H. P., Beard, J. H., and Jeffords, R. M., 1975. Cenozoic planktonic foraminiferal zonation and characteristics of index forms. *Univ. Kansas Paleontol. Contrib.*, 62.

Strickland, J.D.H., and Parsons, T. R., 1968. A manual for seawater analysis. *Bull. Fish. Res. Bd. Canada*, 167:311.

Timur, A., and Toksoz, M. N., 1985. Fundamentals of Well Log Interpretation. *Ann. Rev. Earth Planet. Sci.*, 13:315–344.

Toumarkine, M., and Luterbacher, H., 1987. Paleocene and Eocene planktic foraminifera. *In* Bolli, H. M., Saunders, J. B., and Perch-Nielsen, K. (Eds.), *Plankton Stratigraphy*: Cambridge (Cambridge Univ. Press), 87–154.

Vacquier, V., 1985. The measurement of thermal conductivity of solids with a transient linear heat source on the plane surface of a poorly conducting body. *Earth Planet. Sci. Lett.*, 74:275–279.

Van Gorsel, J. T., and Troelstra, S. R., 1981. Late Neogene planktonic foraminiferal biostratigraphy and climatostratigraphy of the Solo River Section (Iava, Indonesia). *Mar. Micropaleontol.*, 6:183–209.

Von Herzen, R. P., and Maxwell, A. E., 1959. The measurement of thermal conductivity of deep-sea sediments by a needle probe method. *J. Geophys. Res.*, 65:1557–1563.

Wentworth, C. K., 1922. A scale of grade and class terms for clastic sediments. *J. Geol.*, 30:377–392.

Zoback, M. D., and Zoback, M. L., 1980. State of stress in the conterminous United States, *J. Geophys. Res.*, 85:6113–6173.

Zoback, M. D., Zoback, M. L., Mount, V. S., Suppe, J., Eaton, J. P., Healy, J. H., Oppenheimer, D., Reasenberg, P., Jones, L., Raleigh, C. B., Wong, I. G., Scotti, O., and Wentworth, C., 1988. New evidence on the state of stress of the San Andreas Fault. *Science*, 238: 1105–1111.

Zoback, M. L., and Zoback, M. D., in press. Tectonic stress field of the continental United States. *In* Pakiser, L., and Mooney, W. (Eds.), *Geophysical Framework of the Continental United States*: Geol. Soc. Am. Mem.

Ms 124A-102